AMERICAN SOCIETY FOR MICROBIOLOGY | mBio®

RESEARCH ARTICLE

Antibiotic Acyldepsipeptides Stimulate the *Streptomyces* Clp-ATPase/ClpP Complex for Accelerated Proteolysis

Laura Reinhardt,[a,b] Dhana Thomy,[a,b] Markus Lakemeyer,[c] Linda Maria Westermann,[a,b] Joaquin Ortega,[d] Stephan A. Sieber,[c] Peter Sass,[a,b] Heike Brötz-Oesterhelt[a,b]

[a]Department of Microbial Bioactive Compounds, Interfaculty Institute of Microbiology and Infection Medicine, University of Tübingen, Tübingen, Germany
[b]Cluster of Excellence–Controlling Microbes to Fight Infections, University of Tübingen, Tübingen, Germany
[c]Department of Chemistry, Technical University of Munich, Garching, Germany
[d]Department of Anatomy and Cell Biology, McGill University, Montreal, Quebec, Canada

Peter Sass and Heike Brötz-Oesterhelt share senior authorship.

ABSTRACT Clp proteases consist of a proteolytic, tetradecameric ClpP core and AAA+ Clp-ATPases. Streptomycetes, producers of a plethora of secondary metabolites, encode up to five different ClpP homologs, and the composition of their unusually complex Clp protease machinery has remained unsolved. Here, we report on the composition of the housekeeping Clp protease in *Streptomyces*, consisting of a heterotetradecameric core built of ClpP1, ClpP2, and the cognate Clp-ATPases ClpX, ClpC1, or ClpC2, all interacting with ClpP2 only. Antibiotic acyldepsipeptides (ADEP) dysregulate the Clp protease for unregulated proteolysis. We observed that ADEP binds *Streptomyces* ClpP1, but not ClpP2, thereby not only triggering the degradation of nonnative protein substrates but also accelerating Clp-ATPase-dependent proteolysis. The explanation is the concomitant binding of ADEP and Clp-ATPases to opposite sides of the ClpP1P2 barrel, hence revealing a third, so far unknown mechanism of ADEP action, i.e., the accelerated proteolysis of native protein substrates by the Clp protease.

IMPORTANCE Clp proteases are antibiotic and anticancer drug targets. Composed of the proteolytic core ClpP and a regulatory Clp-ATPase, the protease machinery is important for protein homeostasis and regulatory proteolysis. The acyldepsipeptide antibiotic ADEP targets ClpP and has shown promise for treating multiresistant and persistent bacterial infections. The molecular mechanism of ADEP is multilayered. Here, we present a new way how ADEP can deregulate the Clp protease system. Clp-ATPases and ADEP bind to opposite sides of *Streptomyces* ClpP, accelerating the degradation of natural Clp protease substrates. We also demonstrate the composition of the major *Streptomyces* Clp protease complex, a heteromeric ClpP1P2 core with the Clp-ATPases ClpX, ClpC1, or ClpC2 exclusively bound to ClpP2, and the killing mechanism of ADEP in *Streptomyces*.

KEYWORDS caseinolytic protease, AAA+ chaperones, Clp-ATPase, ClpP, ADEP, antimicrobial agents, mode of action

Streptomycetes are known for their complex developmental life cycle as well as for the multitude of secondary metabolites they produce, including important clinically used antibiotics. Morphological differentiation of the filamentous, multicellular bacteria is shaped by a variety of differentiation processes, which include the reorganization of chromosome segregation, cell division, and cell-wall assembly, as well as the formation of a sporulating aerial mycelium (1). In addition, morphological differentiation is coordinated with the extraordinary diverse secondary metabolism. Such complex developmental programs often rely on the activation or inactivation of regulators that may be conferred by transcriptional control, protein modifications, and/or regulated proteolysis. Energy-dependent degradation of

Editor Gerard D. Wright, McMaster University

Address correspondence to Heike Brötz-Oesterhelt, heike.broetz-oesterhelt@uni-tuebingen.de.
The authors declare no conflict of interest.

This work is dedicated to Philippe Mazodier in memoriam of his pioneering work on *Streptomyces* ClpP.

Received 19 May 2022
Accepted 9 September 2022
Published 26 October 2022

short-lived regulators is one essential feature of the compartmentalized, tightly regulated bacterial caseinolytic protease Clp (2), which is intimately involved in the morphological differentiation of *Streptomyces* (3–6).

The Clp protease typically consists of a barrel-shaped, tetradecameric ClpP core that associates with hexameric ATP-consuming unfoldases, so-called Clp-ATPases, for protein degradation (7). The tetradecameric ClpP core is built of two stacked heptameric rings to form the proteolytic chamber of the Clp protease, keeping the catalytic site residues (Ser97, His122, Asp171 in *Escherichia coli*) within the inner lumen of the barrel and away from the cytoplasm (8). Access to the proteolytic chamber is tightly regulated. To prevent undesired substrate degradation, substrate entry is only allowed via two axial pores, which are too small for protein passage. Consequently, in the absence of a cognate Clp-ATPase, ClpP lacks proteolytic activity and only degrades short peptides (9, 10). For regulated proteolysis, Clp-ATPases and associated adaptor proteins recognize natural Clp protease substrates, bind to the apical and/or distal surface of the ClpP core, and unfold and translocate the protein substrates under ATP consumption through the entrance pores into the proteolytic chamber of ClpP (11).

Many bacterial species encode only a single ClpP homolog, thus forming homotetradecameric ClpP complexes, for instance, the model bacteria *E. coli* and *Bacillus subtilis* or pathogens like *Staphylococcus aureus* and *Streptococcus pneumoniae* (8, 12–14). Other pathogenic bacteria, including mycobacteria, chlamydia, listeria, clostridia, and pseudomonads, possess two ClpP isoforms, i.e., ClpP1 and ClpP2, which may form homotetradecameric complexes of either ClpP1 or ClpP2 or heterotetradecameric complexes involving both ClpP homologs (15–20). Streptomycetes have an even more complex Clp system and mostly encode three or five ClpP homologs. Current knowledge of the *Streptomyces* Clp machinery is mainly based on studies using *Streptomyces lividans* cells. In this species, five *clpP* genes are organized in two bicistronic (*clpP1clpP2* and *clpP3clpP4*) and one monocistronic (*clpP5*) operon (3, 21), whose expression was shown to be tightly controlled via several negative feedback loops (22–25). For example, in *S. lividans* wild-type cells, the degradation of the transcriptional activators ClgR and PopR depends on the presence of ClpP1 and ClpP2 (Fig. 1A). Here, ClgR induces the expression of ClpP1 and ClpP2, while the ClgR paralogue PopR is assumed to recruit the RNA polymerase for *clpP3clpP4* transcription. As PopR was shown to be degraded by ClpP1 and ClpP2 in *Streptomyces* cells, PopR-mediated expression of the *clpP3clpP4* operon is silenced in the presence of these two ClpP homologs (21–24). On the other hand, ClpP3 and ClpP4 are expressed in *clpP1clpP2* deletion mutants due to the repealed degradation of PopR (21). In contrast to *E. coli* or *B. subtilis*, where the function of ClpP is not essential for survival, at least one functional copy of either *clpP1clpP2* or *clpP3clpP4* is essential for the viability of *S. lividans* (21). Thus, at least some functional redundancy seems to exist between the ClpP homologs in *Streptomyces* that might represent a rescue mechanism in case the function of ClpP1 and ClpP2 is disturbed or inhibited.

Despite the importance of the Clp system for streptomycetes, data on the exact molecular function of their Clp protease complex is scarce. In the current study, we set out to reconstitute and characterize the Clp system of *Streptomyces hawaiiensis* NRRL 15010 *in vitro*, which has the same *clpP* operon organization as *S. lividans* (26). *S. hawaiiensis* is of particular interest since it is the producer of antibiotic acyldepsipeptide 1 (ADEP1), the natural product progenitor of the potent class of ADEP antibiotics that bind to and deregulate the Clp protease complex (26–31).

We here present the molecular composition of the housekeeping Clp protease in *Streptomyces*, which consists of a heterotetradecameric ClpP1P2 core that interacts with corresponding Clp-ATPases solely via ClpP2. It is the first report on the full *Streptomyces* Clp protease machinery operating *in vitro*, including two ClpP isoforms and three Clp-ATPases working together to degrade natural Clp protease substrates as well as model substrates. In addition, our data assign a new, yet unprecedented mechanism of action to ADEP antibiotics, which is the accelerated degradation of natural

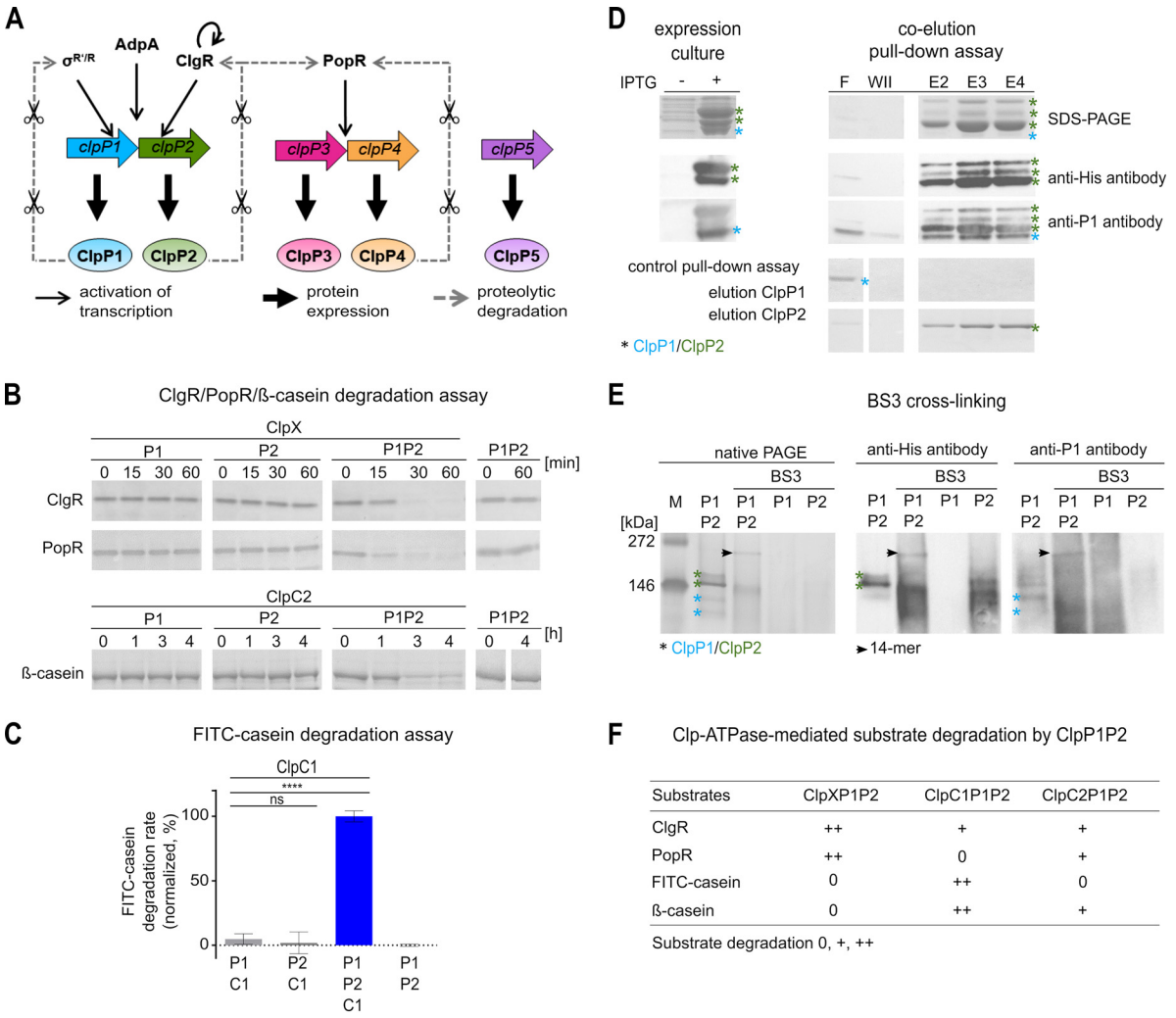

F Clp-ATPase-mediated substrate degradation by ClpP1P2

Substrates	ClpXP1P2	ClpC1P1P2	ClpC2P1P2
ClgR	++	+	+
PopR	++	0	+
FITC-casein	0	++	0
ß-casein	0	++	+

Substrate degradation 0, +, ++

FIG 1 ClpP1 and ClpP2 form a heterotetradecameric core that interacts with the Clp-ATPases ClpX, ClpC1, and ClpC2 for protein degradation. (A) Clp protease-dependent regulatory network in *Streptomyces*. (B and C) *In vitro* protein degradation assays with purified Clp proteins indicate that the hydrolysis of protein substrates depends on the presence of ClpP1, ClpP2, and a partner Clp-ATPase. SDS-PAGE analyses of the degradation of the putative natural Clp substrates ClgR and PopR show that ClpX-mediated degradation of both substrates requires the presence of both ClpP1 and ClpP2 (B). Similarly, both ClpP1 and ClpP2 were required for ClpC2- or ClpC1-dependent digestion of β-casein (B) or FITC-casein (C), respectively. The hydrolysis of FITC-casein was recorded as an increase in fluorescence intensity (relative fluorescence units [RFU]) over time. Mean values (normalized to %) of initial linear reaction kinetics are given. Statistical analyses were performed with one-way ANOVA by using three biological replicates, each comprising three technical replicates. $P > 0.05$, nonsignificant (ns); ****, $P \leq 0.0001$. Error bars indicate standard deviations. For SDS-PAGE images, representative examples of three replicates are shown. (D) Coelution of untagged ClpP1 and His_6-tagged ClpP2 during Ni-NTA chromatography implies the interaction of the two ClpP homologs. Samples of the flowthrough (F), the second wash fraction (WII), and the elution fractions E2–E4 are depicted. The cell lysate used for chromatography was generated after coexpression of ClpP1 (blue asterisk) and ClpP2-His_6 (green asterisks) from two distinct, IPTG-inducible T7 promoters in the pETDUET-vector system. SDS-PAGE and immunoblot using specific anti-His_6 or anti-ClpP1 antibodies are shown. The three observed bands marked by the anti-His_6 antibody correspond to full-length ClpP2 and processed variants (as discussed in a later section). Of note, the polyclonal anti-ClpP1 antiserum cross-reacted with ClpP2, which resulted in the detection of the same three bands as seen with the anti-His_6 as well as an additional band that corresponds to ClpP1. Flowthrough (F) and second wash fraction (W II) of the affinity chromatography experiment indicate the clearance of unbound ClpP1. In a control pulldown experiment, untagged ClpP1 and 6his-tagged ClpP2 were applied separately to a Ni-NTA column. Here, ClpP1 was only detected in the flowthrough fraction (F), whereas ClpP2 was only detected in the elution fractions (E2–E4), thus proving the stringency of the pulldown assay. Assays were performed at least in triplicates, and representative SDS-PAGE images are shown. (E) Cross-linking experiments visualize the heteromeric ClpP1P2 complex. Employing the chemical cross-linker BS3, a protein band with the approximate size of a ClpP tetradecamer appeared only in samples containing both ClpP1 and ClpP2. This band was detected with anti-ClpP1 as well as anti-His_6 antibodies. A sample containing both ClpP1 and ClpP2 in the absence of BS3 did not yield the tetradecamer band, suggesting rather transient interactions between ClpP1 and ClpP2. Assays were performed at least in triplicates, and representative native PAGE images are shown. (F) Overview of Clp-ATPase mediated substrate degradation experiments in combination with the proteolytic core ClpP1P2. Compare also degradation assays in Fig. S1. 0, +, ++ reflect the efficiency of substrate degradation by the distinct Clp protease, respectively.

Clp protease substrates as a result of the concomitant binding of ADEP and Clp-ATPase to opposite sides of the ClpP core.

RESULTS

A heterotetradecameric ClpP1P2 complex interacts with ClpX, ClpC1, and ClpC2 for protein degradation. To investigate the composition and molecular function of the *Streptomyces* Clp protease *in vitro*, we first cloned, heterologously expressed, and purified the *S. hawaiiensis* Clp proteins ClpP1 and ClpP2, their corresponding Clp-ATPase proteins ClpX, ClpC1, and ClpC2, as well as the predicted natural Clp protease substrates ClgR and PopR. We then performed *in vitro* degradation experiments by testing different combinations of ClpP and Clp-ATPase proteins to attempt the digestion of the natural substrates ClgR and PopR as well as the model protein substrates FITC-casein and β-casein, respectively. Our data show that neither ClpP1 nor ClpP2 alone was capable of protein degradation in the presence of a Clp-ATPase (Fig. 1B and C). However, when ClpP1, ClpP2, and Clp-ATPase were used in combination, protein substrates were rapidly digested, thus indicating that both ClpP1 and ClpP2 are required for Clp-ATPase-dependent protein degradation. Of note, not all protein substrates were degraded by all Clp-ATPase combinations or with similar efficiency. When we tested the degradation of ClgR and PopR by ClpP1 plus ClpP2 in the presence of either ClpX, ClpC1, or ClpC2, we observed that the presence of ClpX or ClpC2 leads to the degradation of both ClgR and PopR, although degradation was notably slower with ClpC2, whereas ClpC1 only conferred the degradation of ClgR but not of PopR (Fig. S1A). The model substrates β-casein and FITC-casein were digested by ClpP1 plus ClpP2 in the presence of either ClpC1 or ClpC2 but not when ClpX was present (Fig. S1B and C).

Apparently, the stimulation of activity upon combining ClpP1 and ClpP2 points to the formation of a heterotetradecameric complex consisting of both ClpP homologs. To investigate a potential direct interaction of ClpP1 and ClpP2, we performed coelution and native PAGE experiments using native ClpP1 and C-terminally His_6-tagged ClpP2. During metal-ion affinity chromatography, ClpP1 was retained on the column by His_6-tagged ClpP2 (Fig. 1D), implying a direct interaction of ClpP1 and ClpP2. However, the interaction within the heteromeric ClpP1P2 complex seemed rather weak, and the complex did not appear on standard native gels. To investigate this interaction further and substantiate the existence of a heterotetradecameric complex, we next performed cross-linking experiments using the chemical cross-linker BS3 to stabilize potential transient and weak interactions between both ClpP homologs. Now, the complex was clearly shown and only the combination of both ClpP1 and ClpP2 allowed for the detection of a tetradecameric complex, as documented by native PAGE and immunoblotting analyses using anti-*Streptomyces* ClpP1 and anti-His_6 antibodies (Fig. 1E). In contrast, when ClpP1 or ClpP2 were used individually, no tetradecameric complexes were observed. Hence, our data show that the proteolytic core of the *Streptomyces* Clp protease consists of a ClpP1P2 heterotetradecameric complex that interacts with the Clp-ATPases ClpX, ClpC1, and ClpC2 for the degradation of protein substrates (Fig. 1F).

ClpP1 confers proteolytic activity to the complex, and ClpP2 interacts with the unfoldases ClpX, ClpC1, and ClpC2. Due to the observed heteromeric nature of the *Streptomyces* ClpP core, which consists of the two distinct homologs ClpP1 and ClpP2, we wondered whether both ClpP1 and ClpP2 equally contribute to Clp-ATPase-dependent proteolysis or whether each homolog may fulfill certain, distinct functions during the degradation process. To approach this question, we first analyzed the catalytic activity of the heterotetradecameric wild-type ClpP1P2 complex compared to combinations with the corresponding catalytic triad mutants $ClpP1_{S113A}$ and $ClpP2_{S131A}$, which had been constructed by replacing the nucleophilic serine moiety of the catalytic triad by an alanine residue via site-directed mutagenesis. Of note, both ClpP1 and ClpP2 of *S. hawaiiensis* comprise canonical Ser-His-Asp catalytic triads, analogous to *S. lividans* and *S. coelicolor* (Fig. S1D), but are different from ClpP1 from *Listeria monocytogenes*. *Listeria* ClpP1 features an uncommon asparagine residue instead of aspartate at position 172 that aligns to an active catalytic triad only when ClpP1 forms a complex with ClpP2 (32). Studying the turnover of the fluorogenic model substrate casein in the presence of *S. hawaiiensis* ClpC1, we observed that a mixed core of ClpP1 and $ClpP2_{S131A}$

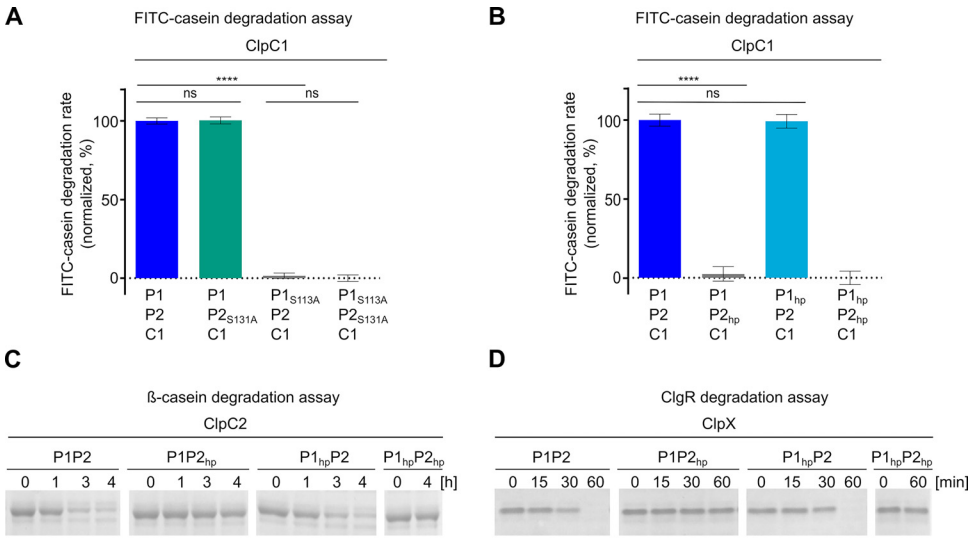

FIG 2 ClpP1 and ClpP2 have different but complementary functions during protein degradation. (A) Impact of mutating the active site serine moieties in the ClpP1P2 heterocomplex. $ClpP1_{S113A}$ but not $ClpP2_{S131A}$ impairs ClpC1-mediated FITC-casein degradation, indicating that substrate protein hydrolysis is conferred by ClpP1. (B) Effect of the hydrophobic pocket mutations in $ClpP1_{hp}$ and $ClpP2_{hp}$ on ClpC1-mediated FITC-casein degradation. Mutations in the hydrophobic pocket of $ClpP2_{hp}$ prevent FITC-casein degradation, while for $ClpP1_{hp}$ degradation is comparable to the wild-type protein, implying that the Clp-ATPase ClpC1 binds via ClpP2. For A and B, the hydrolysis of FITC-casein was recorded as RFU increase over time. Mean values (normalized to %) of initial linear reaction kinetics of the degradation curves are shown. *P* values were calculated with one-way ANOVA using three biological replicates each comprising three technical replicates. ns, $P > 0.05$; ****, $P \leq 0.0001$. Error bars indicate standard deviations. (C and D) Effects of the hydrophobic pocket mutations on ClpC2-mediated degradation of β-casein (C) and ClpX-mediated degradation of ClgR (D). SDS-PAGE analyses show that protein degradation is inhibited in samples harboring the hydrophobic pocket mutant $ClpP2_{hp}$, whereas samples with $ClpP1_{hp}$ retain wild-type activity, indicating that the Clp-ATPases ClpC2 and ClpX also interact via ClpP2. All assays were performed at least in triplicates, and representative SDS-PAGE images are shown.

retained full proteolytic activity at the level of wild-type ClpP1P2 (Fig. 2A). This was in clear contrast to the mixed complexes $ClpP1_{S113A}P2$ or $ClpP1_{S113A}P2_{S131A}$, in which protease activity was abolished for both, thus showing that the catalytic activity of the Clp complex is essentially conferred by ClpP1.

Aside from catalytic activity, the interaction with partner Clp-ATPases, which unfold and feed protein substrates into the ClpP degradation chamber, is a prerequisite for the proteolytic activity of the Clp protease. Therefore, we also probed the interaction of ClpP1 and ClpP2 with the cognate Clp-ATPases by generating particular hydrophobic pocket mutations, which had previously been shown to abrogate Clp-ATPase binding to the ClpP core in the related *M. tuberculosis* (MtClpP) (33). The corresponding three conserved aromatic residues (Y74, Y76, and F96) in the crystal structure of *E. coli* ClpP (EcClpP) are also important for stabilizing Clp-ATPase interactions with ClpP (8), and the same positions were also shown to be involved in the binding of ADEP to *E. coli* and *B. subtilis* ClpP (34, 35). By aligning the protein sequences of *S. hawaiiensis* and *S. lividans* ClpP1 and ClpP2 with EcClpP and MtClpP1P2 (Fig. S1D and E), we identified the corresponding amino acid positions in both *Streptomyces* ClpP1 and ClpP2. To abrogate potential Clp-ATPase/ClpP interactions, but avoid substantial interference with protein structure and folding, suitable amino acids for exchange were selected according to the physicochemical properties and size of the amino acids, i.e., the bulky, aromatic tyrosine was replaced by a valine, whereas the smaller, hydrophilic serine was replaced by an alanine, yielding the hydrophobic pocket mutant proteins $ClpP1_{hp}$ (Y76V, Y78V, and Y98V) and $ClpP2_{hp}$ (S94A, Y96V, and Y116V) (Fig. S1D and E). When different combinations of wild-type and hydrophobic pocket mutant proteins of ClpP1 and ClpP2 were used in *in vitro* degradation assays, it emerged that protein substrates were only digested in the presence of wild-type ClpP2, no matter which of the three ATPases was tested (Fig. 2B to D). Mutagenesis of the ClpP2 hydrophobic pocket

residues resulted in complete inhibition of substrate turnover. In contrast, the corresponding mutations in $ClpP1_{hp}$ did not affect protein degradation, and substrate turnover was comparable to the wild-type protein, indicating that the partner Clp-ATPases bind to the heterotetradecamer exclusively via ClpP2. Hence, our data clearly show that ClpP1 and ClpP2 of the heterotetradecameric ClpP core fulfill separate but complementary functions in the degradation process. ClpP1 confers catalytic activity to the complex, while ClpP2 is essential for the necessary interaction with the partner Clp-ATPases.

ADEP antibiotics induce oligomerization and proteolytic activation of ClpP1 but not of ClpP2. *S. hawaiiensis* is the producer of the natural product antibiotic ADEP1 (Fig. 3A) (26), and Mazodier and colleagues (36) demonstrated in a previous *S. lividans* cell study that ClpP1 is targeted by this antibiotic. We therefore set out to further investigate the effect of ADEP antibiotics on the Clp system of the producer genus and to characterize the potential deregulation of the *in vitro* peptidase and protease activity of *S. hawaiiensis* ClpP1 and ClpP2 in the presence of ADEP1. To do so, we first used the fluorogenic dipeptide Suc-Leu-Tyr-aminomethylcoumarin (Suc-LY-AMC) as a substrate in peptidase activity assays and measured the fluorescence signal that results from peptide cleavage and concomitant AMC release. Our results showed that neither ClpP1, ClpP2, nor ClpP1P2 possessed notable peptidase activity in the absence of ADEP1. However, ADEP1 clearly induced the hydrolysis of Suc-LY-AMC by either ClpP1 alone or by the mixed complex ClpP1P2 but not by ClpP2 alone (Fig. 3B and C). Corroborating our results above, peptidase activity was lost in all assays when ClpP1 was replaced by the active site mutant protein $ClpP1_{S113A}$, while replacing ClpP2 by $ClpP2_{S131A}$ had no effect on the activity of mixed complexes (Fig. 3B). A similar result was observed, when Z-GGL-AMC, Ac-WLA-AMC, or Ac-Ala-hArg-2-Aoc-ACC was used as the substrate in peptidase activity assays (Fig. 3D), although some peptidase activity of ClpP1P2 was notable when using Ac-WLA-AMC in the absence of ADEP1. Probing the binding site, ADEP1 failed to induce peptide hydrolysis when ClpP1 was exchanged by the hydrophobic pocket mutant protein $ClpP1_{hp}$, whereas replacement of ClpP2 by $ClpP2_{hp}$ had no effect on substrate hydrolysis by the mixed complex (Fig. 3B). These results indicate that ADEP1 interacts with ClpP1, but not with ClpP2. Thermal shift assays confirmed the binding affinity of ClpP1 toward ADEP1, demonstrated by an increase of >16°C in the melting temperature of the homotetradecamer in combination with ADEP1. In contrast, ADEP1 could not increase the melting temperature of ClpP2, hereby confirming that ClpP2 does not interact with ADEP1 (Fig. 3E and Fig. S2A). Such observed asymmetric binding was not restricted to ADEP1 but was also detected for ADEP2 and ADEP4, two synthetic derivatives previously optimized for potent anti-*S. aureus* activity (27). Uniformly, all tested ADEPs induced peptidase activity via binding to ClpP1 but not to ClpP2 (Fig. 3B and F). Interestingly, ClpP1P2 exhibited slightly higher peptidase activity when activated by ADEP1, compared to ADEP2 and ADEP4, thereby indicating that the binding of the natural compound ADEP1 to *Streptomyces* ClpP1 may have been evolutionarily optimized. Mixed ClpP1P2, $ClpP1P2_{S131A}$, and $ClpP1P2_{hp}$ exhibited superior peptidase activity in the presence of ADEP1 compared to ClpP1 alone (Fig. 3B), implying a stimulation of ClpP1 catalytic activity by the interaction with ClpP2. Of note, the presence of ADEP-ClpP1P2 complexes was verified by native PAGE and size exclusion chromatography (Fig. S2B to F). Similar results were observed in protease activity assays using fluorogenic FITC-casein as a substrate and measuring FITC release upon casein degradation (Fig. 3G). In addition, here, ADEP1 induced proteolysis of casein by either ClpP1 alone or by mixed ClpP1P2 but not by ClpP2, and again the mixed complex performed better than ClpP1 alone. Thus, our data reveal that ADEP1 activates the purified and otherwise dormant *Streptomyces* ClpP core to Clp-ATPase-independent peptidase and protease activity by binding to and deregulating the activity of ClpP1.

Next, we analyzed the oligomeric states of ClpP1 and ClpP2 in the absence and presence of ADEP1 by size exclusion chromatography (Fig. 3H). Regarding ClpP1, it emerged that the addition of ADEP1 clearly led to a distinct shift of the peak representing a ClpP1

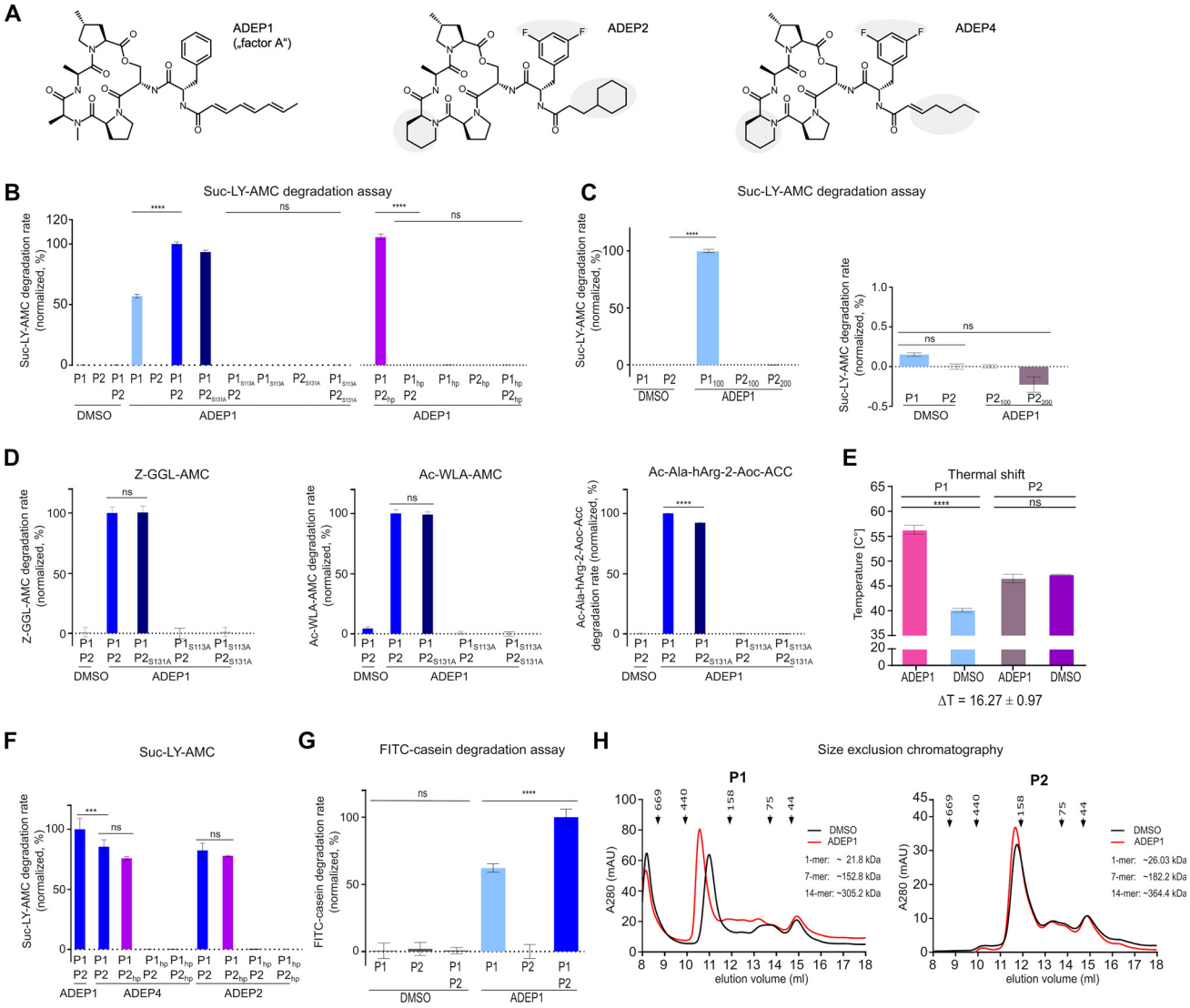

FIG 3 ADEP binds to and deregulates ClpP1 but not ClpP2. (A) Chemical structures of the natural product ADEP1 and its synthetic congeners ADEP2 and ADEP4. ADEP1, representing "factor A" of the A54556 antibiotic complex produced by *S. hawaiiensis* NRRL 15010, consists of a macrolactone core, an aliphatic side chain, and an *N*-acylphenylalanine linker. Differences in the chemical structures between these ADEP derivatives are indicated in gray. (B to E) Effect of ADEP on the peptidase activity of ClpP1 and ClpP2. Peptidase activity assays using the fluorogenic dipeptide Suc-LY-AMC as the substrate show that in the absence of ADEP1 (DMSO controls), ClpP1 and ClpP2 alone or combined are devoid of peptidase activity. (B) Addition of ADEP1 triggered peptidase activity of ClpP1 alone and, even stronger, of the ClpP1P2 heterocomplex, while ClpP2 alone remained inactive. Peptide hydrolysis was prevented in samples containing the catalytic triad or hydrophobic pocket mutant proteins $ClpP1_{S113A}$ or $ClpP1_{hp}$, respectively, but not in the corresponding ClpP2 mutants, thus indicating ADEP1 binding via ClpP1. The slopes of initial degradation rates are shown, normalized in %. (C) Elevated concentrations of ADEP1 (100 μM or 200 μM) did not lead to detectable peptidase activity of ClpP2 (4 μM). ClpP1 served as a positive control. The slopes of initial degradation rates are shown (normalized in %; ClpP1 activity set to 100%). The right panel is the magnified area near the baseline (*y* axis from −0.5% to 1%). ClpP1 activity without ADEP is only 0.15% of the ClpP1 activity in the presence of ADEP. (D) Peptidase assays using the fluorogenic peptide substrates Z-GGL-AMC, Ac-WLA-AMC, and Ac-Ala-hArg-2-Aoc-Acc confirm that peptidase activity is mediated by ClpP1 but not by ClpP2. (E) Thermal shift assays confirmed the binding affinity of ClpP1 toward ADEP1, demonstrated by an increase of 16.27°C in the melting temperature of the homotetradecamer in combination with ADEP1. In contrast, ADEP1 could not increase the melting temperature of ClpP2, hereby confirming that ClpP2 does not interact with ADEP1. (F) Peptidase assays using the derivatives ADEP2 and ADEP4 in comparison to ADEP1. The data indicate that asymmetric binding to ClpP1 is not restricted to ADEP1 but occurs also for ADEP2 and ADEP4. Of note, ClpP1P2 exhibited slightly higher peptidase activity in the presence of ADEP1 compared to ADEP2 and ADEP4. (G) Effect of ADEP1 on the protease activity of ClpP1 and ClpP2 using FITC-casein as a substrate. ADEP1 activated casein degradation by ClpP1 alone and even more by the ClpP1P2 heterocomplex, while ClpP2 alone remained inactive. DMSO was used in control reactions. Mean values (normalized to %) of initial linear reaction kinetics are given. In B to F, error bars represent standard deviations. Statistical analyses were performed with one-way ANOVA using three biological replicates each comprising three technical replicates, except for the Suc-LY-AMC degradation assays with the hydrophobic pocket mutants $ClpP1_{hp}$ and $ClpP2_{hp}$, where two biological replicates were used. ns, $P > 0.05$; ****, $P \leq 0.0001$. Error bars indicate standard deviations. (H) Oligomeric state analyses of native ClpP1 and native ClpP2 as determined by size exclusion chromatography. ADEP1 triggered the shift of the ClpP1 peak, potentially indicating a transformation from the compressed form of the ClpP1 tetradecamer to its active, extended form, which would explain the independent peptidase and protease activity of ADEP1-activated ClpP1. In contrast, the peak of ClpP2 did neither significantly shift nor form homotetradecamers in the presence of ADEP1. DMSO was used as a control. Depicted experiments are representatives of three biological replicates.

tetradecamer (calculated molecular mass of 305.2 kDa), potentially shifting an existing compressed form of the ClpP1 tetradecamer to its active, extended form. In contrast, the elution profile of ClpP2 did not change in the presence of ADEP1, and ClpP2 mainly eluted as heptamers (calculated molecular mass of 182.2 kDa) or lower oligomeric species, while ClpP2 tetradecamers (calculated molecular mass of 364.4 kDa) were not detected (Fig. 3H). Hence, our data show that ADEP1 binds to ClpP1 and triggers its oligomerization into catalytically active ClpP1 tetradecamers. This explains the independent peptidase and protease activity of ClpP1 in the presence of ADEP1, while ClpP2 does not appear to interact with ADEP1 under the conditions tested.

In line with this, it is noteworthy that the ClpP1 and ClpP2 proteins underwent processing reactions in the course of our *in vitro* degradation experiments (Fig. S3 and S4). *In vitro*, processing of ClpP1 relied either on the binding of ClpXP2 or on the binding of ADEP (regardless of ClpP2), while processing of ClpP2 strictly depended on the presence of ClpP1 but not on ClpX or ADEP (Fig. S3A and B). However, the processing of both ClpP1 and ClpP2 fully relied on the integrity of the catalytic triad of ClpP1 (Fig. S3C) and did not alter the requirement of heterotetradecameric complexes for proteolytic activity (Fig. S4F), thereby corroborating our hitherto obtained results.

Differences in the binding pocket of ClpP1 versus ClpP2 modulate specificity to ADEP and ClpC1. Since ADEP and Clp-ATPases usually bind to the same hydrophobic pockets of the ClpP barrel, it is intriguing that ClpP1 emerged ADEP-sensitive but did not interact with Clp-ATPases, whereas ClpP2 was ADEP insensitive while constituting the main interaction partner for ClpX, ClpC1, and ClpC2. When analyzing the hydrophobic pockets of ClpP1 and ClpP2, it became apparent that both isoforms differ in the first amino acid residue that was selected for mutation of each ClpP hydrophobic pocket (Y76 in ClpP1 and S94 in ClpP2, see above). Since tyrosine and serine obviously differ regarding their size and physicochemical properties, we hypothesized that this difference may influence the binding capability of ClpP1 versus ClpP2 for ADEP and corresponding Clp-ATPases. We therefore exchanged Y76 of ClpP1 by a serine and, vice versa, S94 of ClpP2 by a tyrosine, thereby yielding the hydrophobic pocket mutant proteins $ClpP1_{Y76S}$ and $ClpP2_{S94Y}$. Native PAGE showed that $ClpP1_{Y76S}$ was notably impaired in ADEP-induced assembly of homotetradecamers (Fig. S2G), and consequently, in the presence of ADEP, $ClpP1_{Y76S}$-containing complexes showed substantially decreased peptidase activity compared to wtClpP1 (Fig. S2H), together indicating that the binding of ADEP to $ClpP1_{Y76S}$ was impaired. Of note, ClpC1-mediated protease activity of $ClpP1_{Y76S}P2$ was also reduced, suggesting that Y76 may also have a role in Clp protease assembly and/or catalysis. Now, probing $ClpP2_{S94Y}$, protease activity of $ClpC1P1P2_{S94Y}$ was significantly reduced, suggesting impaired interaction of ClpC1 with $ClpP2_{S94Y}$. However, the $ClpP2_{S94Y}$ mutation did not suffice to make ClpP2 responsive to ADEP (peptidase activity could not be activated by ADEP). Thus, our results clearly indicate that Y76 in ClpP1 and S94 in ClpP2 play crucial roles in conferring the specificity to ADEP versus ClpC1, respectively. However, switching Y76 in ClpP1 and S94 in ClpP2 was not sufficient to switch the individual binding specificities regarding ADEP and ClpC1 entirely, which may be due to the individual protein characteristics of both ClpP1 and ClpP2, e.g., intramolecular bonds, folding characteristics, cavity spacing, and/or further potentially contributing amino acids.

Cell-based studies corroborate the existence of a heteromeric, asymmetric Clp protease complex in *Streptomyces*. Our study so far employed purified *S. hawaiiensis* proteins *in vitro* to elucidate the molecular composition and function of the *Streptomyces* Clp protease. To verify our findings on the level of the *Streptomyces* cell and to also transfer these findings to other *Streptomyces* strains, we chose *S. lividans* as a model strain for confirmative experiments, since earlier studies on the Clp system in streptomycetes were focused on this organism (21–23, 26, 36). In this context, it is noteworthy, that ClpP1 and ClpP2 of *S. hawaiiensis*, *S. lividans*, and *S. coelicolor* appear closely related and share high sequence similarity (Fig. S1D). To this end, we constructed in-frame Δ*clpP1* (Δ*SlP1*) as well as Δ*clpP1clpP2* (Δ*SlP1P2*) deletion mutants in *S. lividans*, which we complemented with either *SlclpP1* or *SlclpP1P2*, respectively. In addition, C terminally His_6-tagged SlClpP2 (SlClpP2-His_6) was

constructed for detection purposes. Cell extracts of the respective deletion and complemented mutants were then analyzed via immunoblotting for the SlPopR-dependent expression of SlClpP3 by utilizing anti-ClpP1, anti-ClpP3, and anti-His_6 antibodies. Here, we regarded the absence of SlClpP3 as a reporter for the functional state of the SlClpP1P2 system, based on previous studies in *S. lividans* (22), which have shown that the degradation of SlPopR by SlClpP1P2-mediated regulatory proteolysis prevents the expression of SlClpP3. In short, whenever SlClpP3 is present, SlClpP1P2 is not capable of degrading SlPopR (Fig. 4A). In line with our *in vitro* results described above, *in vivo* SlClpP1P2 protease activity (and the corresponding absence of SlClpP3) could only be observed, when both SlClpP1 and SlClpP2 were present in the cell (Fig. 4B and Fig. S5A), thus underlining the requirement of a functional interaction of ClpP1 and ClpP2.

We then explored ClpP catalytic triad mutant proteins in *S. lividans* by complementing the Δ*SlP1P2* mutant with different combinations of the wild-type and serine-to-alanine mutant genes *SlclpP1*$_{S113A}$, *SlclpP2*$_{S132A}$, and *SlclpP2*$_{S132A}$*-His* (Fig. 4B and Fig. S5B). Here, immunoblotting experiments showed that a SlClpP1P2 system capable of SlPopR degradation depends on a functional catalytic triad in SlClpP1, but not in SlClpP2, thus supporting our *in vitro* results and providing first *in vivo* evidence that the catalytic function of ClpP1 accounts for the proteolytic activity of the heteromeric ClpP1P2 complex in *Streptomyces*.

We next investigated the binding of Clp-ATPases to the SlClpP1P2 complex in *S. lividans* cells by complementing the Δ*SlP1P2* mutant with different combinations of the wild-type and hydrophobic pocket mutant proteins $SlClpP1_{hp}$, $SlClpP2_{hp}$, and $SlClpP2_{hp}$-His (Fig. 4B and Fig. S5C). The degradation of SlPopR, and thus the presence of a SlClpP1P2 system capable of hydrolyzing protein substrates, depended on a functional hydrophobic pocket in SlClpP2 but not in SlClpP1, therefore corroborating our *in vitro* results that Clp-ATPase binding occurs via ClpP2, but not via ClpP1. Regarding the binding of ADEP to the SlClpP1P2 complex, we conducted disk diffusion bioassays to determine the effect of the respective deletions and complementations on ADEP sensitivity (Fig. 4C). Here, ADEP sensitivity entirely relied on the presence of a functional SlClpP1 protein but not on SlClpP2, thus verifying the exclusive binding of ADEP to ClpP1 and indicating that a functional ClpP1 protein is sufficient to unleash the antimicrobial activity of ADEP in *Streptomyces*.

ADEP antibiotics accelerate the Clp-ATPase-dependent hydrolysis of protein substrates by the *Streptomyces* Clp protease. Our data provides *in vitro* and cell-based evidence that *Streptomyces* ClpP1 and ClpP2 form a heterotetradecameric complex that can be activated for proteolytic activity either by a cognate Clp-ATPase via ClpP2 or by the small molecule antibiotic ADEP1 via ClpP1. Previous studies on Clp proteases from other bacteria, such as *B. subtilis*, *S. aureus*, *E. coli*, *M. tuberculosis*, and *Chlamydia trachomatis*, demonstrated that the addition of ADEP to a reaction mixture of ClpP and a Clp-ATPase abrogated the interaction between the Clp-ATPase and the ClpP core in all cases and consequently prevented Clp-ATPase-dependent substrate hydrolysis without exception (19, 37–40). This steric competition led to the inhibition of the natural functions of the Clp protease in these bacteria. Intrigued by our observation that the *Streptomyces* Clp-ATPases and ADEP interact with separate ClpPs, we wanted to know if the situation might be different in this genus. First, we compared *in vitro* protein degradation of the native substrates ClgR and PopR by ClpXP1P2 in the absence or presence of ADEP1. While ClgR and PopR were digested by ClpXP1P2 in the absence of ADEP (Fig. 1B and 2D), the addition of ADEP did not prevent the degradation of both substrates but, on the contrary, even led to a weak but notable increase of substrate digestion over time (Fig. 5A and E). In addition, the ClpC1P1P2-mediated degradation of PopR was markedly stimulated by ADEP (Fig. S6A). Of note, natural substrate degradation did not occur in the absence of a Clp-ATPase or with the hydrophobic pocket mutant protein $ClpP2_{hp}$ (Fig. 5A and E), indicating that the interaction with a Clp-ATPase remains a prerequisite for the digestion of natural Clp substrates and excluding Clp-ATPase-independent digestion of both substrates via ADEP-activated ClpP1P2.

To further study the unprecedented acceleration of the Clp-ATPase-dependent substrate hydrolysis by ADEP, we tested the effect of ADEP1 on the degradation of the protein

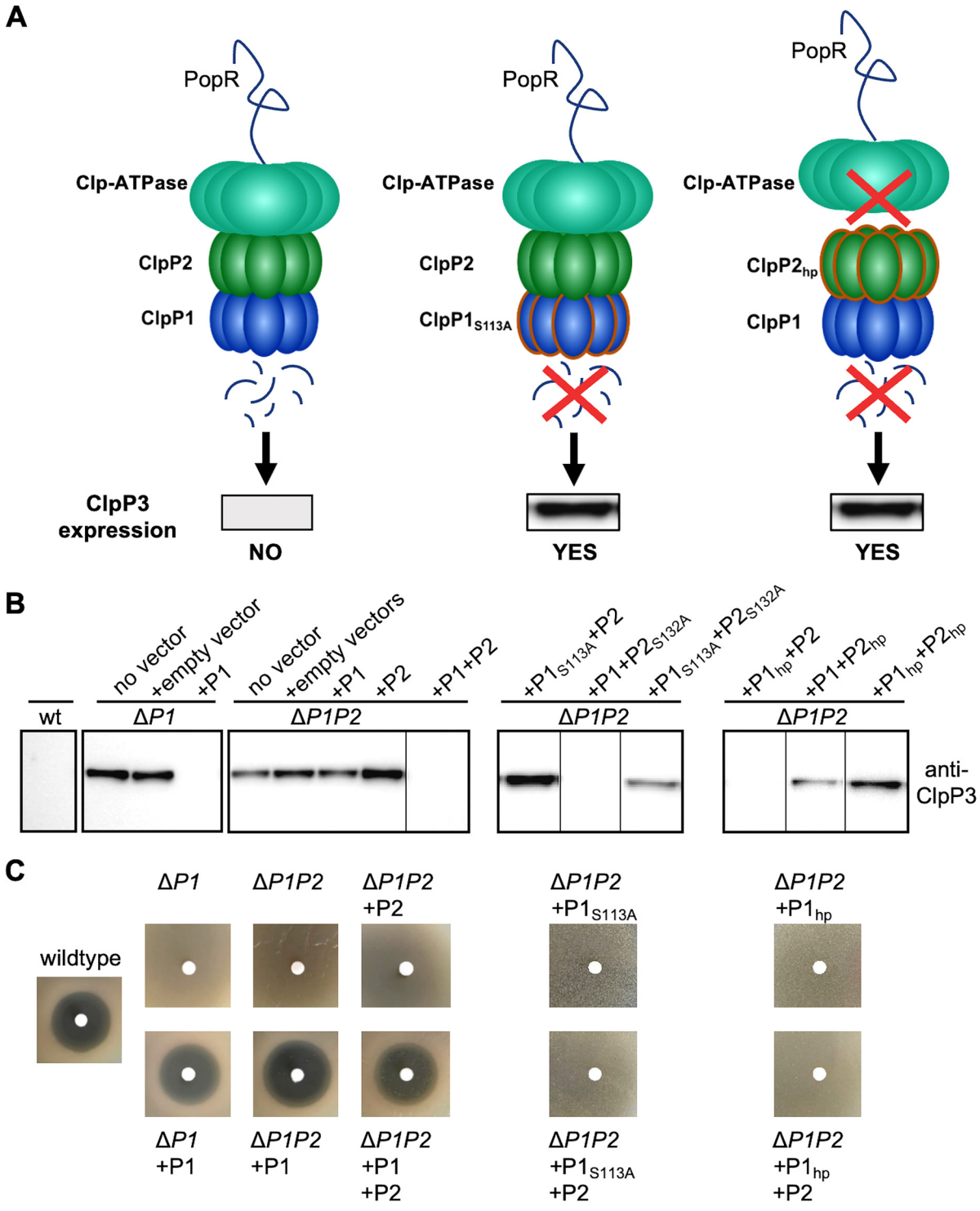

FIG 4 Cell-based studies verify the presence of a heteromeric ClpP1P2 complex, Clp-ATPase binding via ClpP2 as well as ADEP binding via ClpP1. (A) Schematic overview of the effect of Clp protease functionalities on ClpP3 expression. (B) Immunoblotting of cell lysates from wild-type and mutant *S. lividans* cells (as indicated) using anti-ClpP3 antibodies. By reconstituting wild-type, catalytic triad mutants, or hydrophobic pocket mutants of SlClpP1 or SlClpP2, our results using *Streptomyces* cells underline the requirement for both SlClpP1 and SlClpP2 to build a functional, heteromeric Clp protease system, which strictly depends on a functional catalytic triad of SlClpP1 for proteolytic activity and on a functional hydrophobic pocket of SlClpP2 for the interaction with corresponding Clp-ATPases (both indicated by the loss of PopR degradation and concomitant expression of SlClpP3 in mutants harboring either $ClpP1_{S113A}$ or $ClpP2_{hp}$, respectively). All assays were performed at least in triplicates. Representative Western Blot images are shown. (C) Disk diffusion bioassay using ADEP1 verifies ADEP binding via ClpP1 in *S. lividans*, since only the loss of a functional copy of SlClpP1, but not of SlClpP2, confers ADEP resistance. Bioassays were performed at least in triplicates. Representative images are shown.

model substrate GFP-ssrA by ClpXP1P2. The ssrA-tag is a common degron that is recognized by Clp-ATPases and results in the subsequent degradation of the fusion protein by the Clp protease (41). The kinetics of GFP-ssrA hydrolysis can be conveniently followed by measuring a decrease in fluorescence (42). In line with our previous results, ADEP1 clearly stimulated GFP-ssrA degradation by ClpXP1P2 (Fig. 5B). Neither ClpP1P2 alone nor ClpX alone, in the absence or presence of ADEP1, could degrade the substrate, demonstrating the strict necessity of a fully assembled Clp protease complex for GFP-ssrA hydrolysis. In our control sample with $ClpXP1_{S113A}ClpP2_{S131A}$, we did not detect a decline in relative fluorescence units (RFU), indicating that the drop in RFU, measured for ClpXP1P2, is due to unfolding and cleavage of the substrate. Similarly, ADEP1 notably induced the degradation of FITC-casein by ClpC1P1P2 (Fig. 5C) and β-casein by ClpC2P1P2 (Fig. 5D). Drawing this conclusion from experiments with casein, which can serve as a substrate for ADEP-activated as well as Clp-ATPase-activated ClpP1P2, is possible by comparing the degradation rates of the individual complexes. Degradation efficacy was the highest when both activators were present at the same time (forming ADEP-ClpP1P2-Clp-ATPase complexes) and significantly lower ($P \leq 0.0001$) for ClpP1P2-Clp-ATPase, ADEP-ClpP1P2, and ADEP-ClpP1 (activity decreasing in that order; Fig. 3G and Fig. 5C to E). The fact that ADEP addition to the ClpP1P2-Clp-ATPase complex further stimulated casein proteolysis speaks against the significant formation of the less active ADEP-only complexes. Further noteworthy, the stimulated Clp-ATPase/ClpP1P2 activity in the presence of ADEP was not due to an increased ATP turnover, since the conversion of ATP to ADP was unchanged in ClpC1-mediated casein degradation assays in the absence and presence of ADEP (Fig. S6B). In summary, our data clearly show that ADEP1 accelerates the Clp-ATPase-driven degradation of protein substrates by the *Streptomyces* housekeeping Clp protease.

Further noteworthy, under these conditions and after β-casein had been fully digested, ClpC2 was slowly degraded as well (Fig. 5D). Similarly, after complete degradation of PopR had occurred and during prolonged incubation, ClpC1 was also degraded in the presence of ADEP1 (Fig. S6A), suggesting ClpC1 and ClpC2 as putative targets of the ADEP-deregulated ClpP protease in *Streptomyces*.

DISCUSSION

Soil-dwelling bacteria of the genus *Streptomyces* are among the most important producers of secondary metabolites, facilitating the production of over two-thirds of all antibiotics in clinical use today (43). Such vast biosynthetic capacity of streptomycetes, which is accompanied by a complex developmental life cycle, clearly requires tight regulation and coordination of the involved processes. Regulated proteolysis has emerged as an important level of regulation that is intricately linked to cell cycle progression and physiological transitions (44). We aimed to study the molecular function of the housekeeping *Streptomyces* Clp protease machinery, an essential compartmentalized protease in *Streptomyces* and a major player of regulated proteolysis in bacteria (3–5, 45). The *Streptomyces* Clp system is one of the most complex known to date, since streptomycetes encode up to five different ClpP homologs and at least four different Clp-ATPases (3, 21). Previous work by Mazodier and colleagues on *S. lividans* cells provided the first important insights into the potential working mode of the *Streptomyces* Clp protease (22, 23). They observed that the presence of ClpP1 and ClpP2 precluded the expression of ClpP3 and ClpP4 and that the presence of both ClpP1 and ClpP2 was necessary for the digestion of PopR or ClgR. Hence, their data suggested the presence of housekeeping Clp proteases with one or more proteolytic cores, consisting of either ClpP1, ClpP2, or even both homologs, as well as a back-up conferred by ClpP3 and/or ClpP4 that takes over the most important cellular functions in case of a dysfunction of the housekeeping Clp machinery.

Almost two decades later, we have now deciphered the composition and molecular operation mode of the housekeeping Clp protease in *Streptomyces* via *in vitro* reconstitution of the protease system side-by-side with corresponding cell-based studies. Here, we prove that the *Streptomyces* housekeeping Clp protease contains a heterotetradecameric,

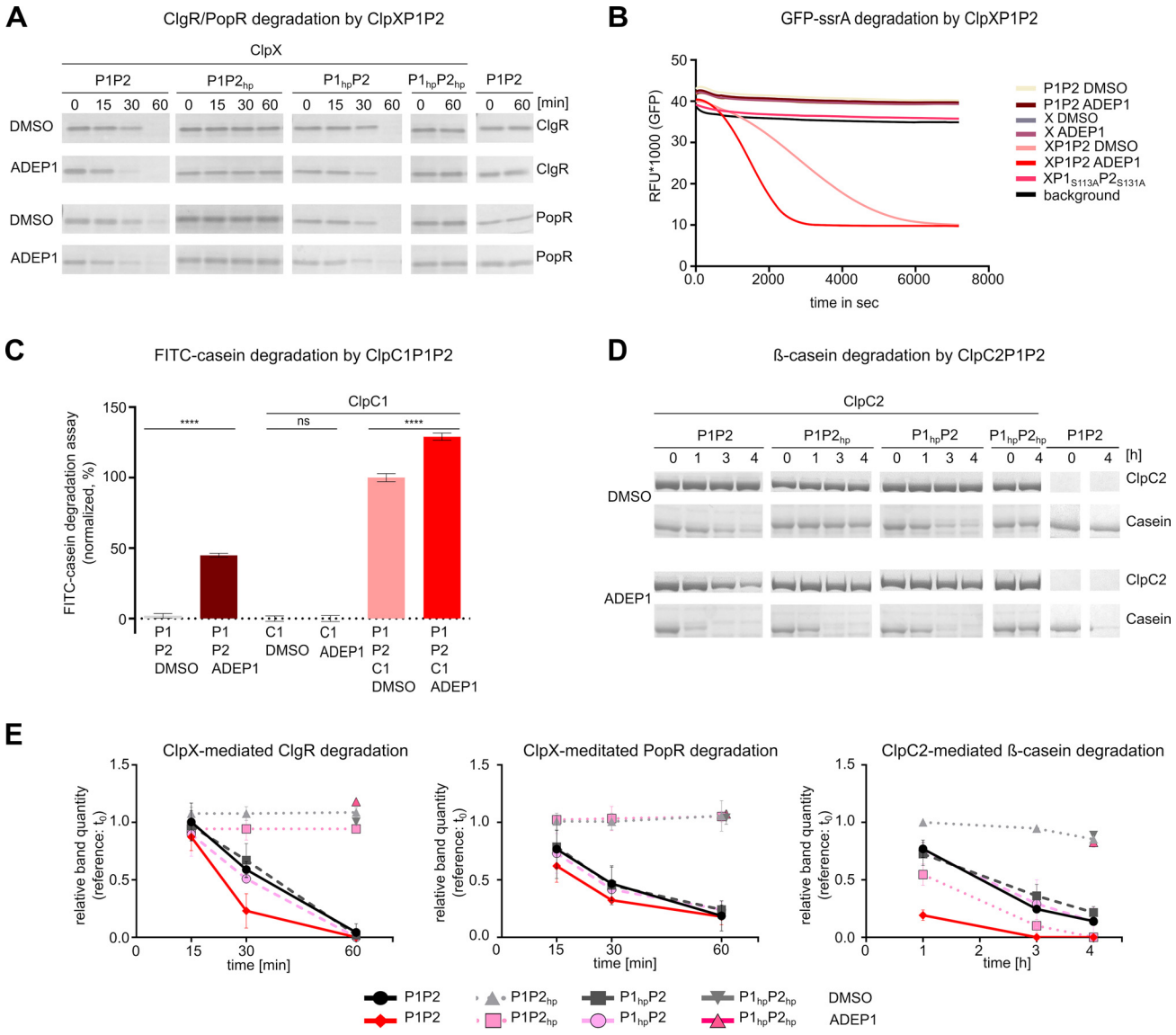

FIG 5 ADEP1 accelerates the proteolytic activity of the *Streptomyces* Clp protease. (A) ADEP accelerates the degradation of the natural Clp substrates ClgR and PopR by ClpXP1P2 in *in vitro* protein degradation assays. Functional ClpX and its interaction with ClpP2 are prerequisites for ClgR and PopR degradation, even in the presence of ADEP. (B) ADEP increases the hydrolysis of GFP-ssrA by ClpXP1P2. GFP-ssrA degradation was measured via fluorescence decrease over time. Background indicates default GFP fluorescence in the buffer solution without enzymes. Data shown are exemplary for at least three biological replicates. (C) ADEP activates the free ClpP1P2 core to degrade FITC-casein and in addition stimulates the ClpC1-mediated FITC-casein degradation. Protease activity assays using FITC-casein as a substrate show that ADEP1 induces FITC-casein degradation by both ClpP1P2 as well as by ClpC1P1P2. Hydrolysis of FITC-casein was monitored as RFU increased over time. Mean values (normalized in %) of initial linear reaction kinetics are shown. *P* values were calculated with one-way ANOVA from three biological replicates each comprising three technical replicates. ns, $P > 0.05$; ****, $P \leq 0.0001$. Error bars indicate standard deviations. (D) ADEP activates the free ClpP1P2 core to degrade β-casein and in addition stimulates the ClpC2-mediated β-casein degradation. ClpC2-mediated β-casein degradation is prevented in the hydrophobic pocket mutant protein $ClpP2_{hp}$. However, ADEP1 can still activate the $ClpP1P2_{hp}$ proteolytic core by binding to ClpP1. Hydrolysis of β-casein is only completely prevented when both hydrophobic pocket mutants, $ClpP1_{hp}$ and $ClpP2_{hp}$, are used in combination. Hydrolysis of β-casein is fastest when wild-type ClpP1P2 interacts with both activators, i.e., ClpC2 plus ADEP, in parallel. Of note, in ADEP-containing reaction mixtures, ClpC2P1P2 degrades β-casein first followed by digestion of ClpC2. All assays were performed at least in triplicates. In SDS-PAGE images, representative experiments are shown. DMSO was used in all control reactions. (E) Densitometry of SDS-PAGE proteins bands of ClgR and PopR (Fig. 5A) and β-casein (Fig. 5D) of each time point relative to the samples collected at t_0. The relative band quantity was measured from three replicate SDS-PAGE analyses. Mean values are shown and error bars indicate corresponding standard deviations. Of note, a slight decrease of the β-casein band in the negative-control $ClpP1_{hp}P2_{hp}$ and $ClpP1P2_{hp}$ could be detected, which might be due to independent unfolding activity of the only partially folded β-casein by ClpC2.

proteolytic core of both ClpP1 and ClpP2 that interacts with the corresponding Clp-ATPases ClpX, ClpC1, or ClpC2 for the degradation of proteins, such as the natural Clp substrates ClgR and PopR. Within the assembled Clp protease variants, we show that ClpP1 and ClpP2 fulfill distinct but complementary functions with regard to substrate hydrolysis.

Our results clearly indicate that mainly ClpP1 confers catalytic activity to the proteolytic core, while ClpP2 is essential for the interaction with the corresponding Clp-ATPases to allow for substrate unfolding and translocation into the degradation chamber of ClpP1P2.

Our data further indicate that the heteromeric ClpP1P2 core is formed by two separate homoheptameric rings of either ClpP1 or ClpP2. Functional Clp-ATPases are hexamers, and all six IGF-loops of *E. coli* ClpX (EcClpX) are required for productive substrate digestion by EcClpXP (46). In that study, even the loss of a single IGF-loop reduced the affinity of EcClpX to EcClpP by approximately 50-fold. In the *Streptomyces* ClpP1P2 core, the mutation of the ClpP1 hydrophobic pocket did not affect the hydrolysis of native substrates at all, which clearly argues against the presence of even a single ClpP1 monomer in the Clp-ATPase-interacting ClpP2 ring. In addition, both *Streptomyces* ClpP1 as well as ClpP2 exist as homoheptamers (as well as homotetradecamers for ClpP1) as revealed by size exclusion chromatography in our study, making the presence of mixed heptamers in the active protease highly unlikely. The presence of two homoheptameric rings of either ClpP1 or ClpP2 in *Streptomyces* further correlates with the composition of the ClpP system in the closely related *M. tuberculosis* (33, 47, 48) and *Mycobacterium smegmatis* (20) as well as *L. monocytogenes* (16, 49), which form heterotetradecamers composed of a ClpP1 heptamer stacked to a ClpP2 heptamer and those complexes bind Clp-ATPases solely via ClpP2.

S. hawaiiensis is the producer of the ClpP-interfering antibiotic ADEP1, the natural product progenitor of a promising class of potent acyldepsipeptide antibiotics (26, 28, 31, 50), and the ADEP mode of action has been investigated in more detail in the major target bacteria. Until now, the effects of ADEP on the housekeeping Clp protease of the producer genus *Streptomyces* have remained mostly elusive. Pioneering cell-based studies by Mazodier and colleagues (36) using the ADEP-sensitive *S. lividans* showed that ClpP1 is a target for ADEP1, since the deletion of the *clpP1* gene conferred ADEP resistance in *S. lividans*. In addition, we have recently reported on the presence of a self-resistance factor in the ADEP producer *S. hawaiiensis* NRRL 15010, which is an accessory ClpP protein with a yet unknown mechanism (26). To obtain further insights into the role of ADEP in *Streptomyces*, we here investigated the effect of ADEP on the molecular function of the housekeeping Clp protease systems of *S. hawaiiensis* and *S. lividans*. Of note, the ClpP1 and ClpP2 proteins of *S. hawaiiensis* show very high amino acid sequence similarities to their corresponding homologs in *S. lividans*, thus suggesting a similar operation mode of ClpP1P2 in both species (Fig. S1D).

Previous studies on the mode of action of ADEP antibiotics have identified two distinct molecular mechanisms that, either together or individually, lead to bacterial killing. Intriguingly, the killing mode depends on the bacterial species and growth environment, and both mechanisms are described as follows. First, since Clp-ATPases and ADEP accommodate the same binding site on ClpP in the species studied so far, the binding of ADEP to ClpP displaces the commonly associated Clp-ATPases from the proteolytic core (19, 37–40). This leads to an inhibition of all physiological functions of the Clp protease in the bacterial cell, including regulated proteolysis. Second, ADEP binding induces an opening of the ClpP entrance pores and allosterically activates the catalytic centers, thereby allowing access of nonnative substrates to the ClpP degradation chamber that are efficiently degraded (19, 30, 34, 35, 38, 51, 52). The latter activation of the independent proteolytic core ClpP is the primary cause of bacterial killing in species harboring nonessential ClpP proteins, such as *B. subtilis* or *S. aureus* (27, 29, 30, 51, 53, 54). However, in an infection situation, where the Clp protease is essential for the expression of important virulence factors, inhibition of the natural functions will also attenuate a pathogen in the host environment (55, 56). In *M. tuberculosis*, the Clp protease is essential for viability under all conditions (48, 57), and we have previously shown that an ADEP-conferred mechanism of Clp protease inhibition leads to cell death in mycobacteria (39). Considering the essentiality of the Clp protease in *Streptomyces* and the comparative phylogenetic closeness to mycobacteria (21), it was thus tempting to hypothesize a mechanism of Clp protease inhibition as the basis of ADEP-dependent killing of *Streptomyces*. To our surprise, ADEP did not abrogate the Clp-ATPase-mediated substrate digestion. All our data consistently show that the presence of

ADEP leads to an unexpected stimulation of the *Streptomyces* Clp protease to digest its natural substrates in a Clp-ATPase-dependent, more efficient manner, rather than leading to an inhibition of its natural functions. Furthermore, ADEP-stimulated Clp-ATPase/ClpP1P2 activity was not due to an increased ATP turnover. Hence, stimulation may be solely attributed to the ADEP effects that are exerted on the structural network of the entire ClpP1P2 complex. This may include adjustment of the active site residues in ClpP1 as well as pore opening for ClpP1 and ClpP2, as was previously described for ADEP-activated ClpP in other bacteria (15, 34, 35, 38). Therefore, the current study reveals a third, yet unobserved, mode of ADEP action.

This new ADEP effect observed here can be explained by our observation that, in *Streptomyces*, the proteolytic ClpP1P2 core can be powered simultaneously by two different activator types. We found ADEP to bind solely to ClpP1 of *S. hawaiiensis* and *S. lividans*. Very recently, asymmetric binding of ADEP to ClpP1 was also observed for ClpP1P2 heterotetradecamers of *Streptomyces cattleya* (58) suggesting that this binding mode is a general characteristic of the genus *Streptomyces*. Furthermore, our *in vitro* and cell-based data consistently reveal that the ClpP2 apical face of the *Streptomyces* ClpP1P2 core serves as the sole docking site for three different Clp-ATPases. The simultaneous and unhindered binding of ADEP and a Clp-ATPase to opposite sides of the *Streptomyces* ClpP core is unique among all the Clp systems investigated so far.

Considering previous studies on ClpP proteins from other bacteria and the effects of ADEP antibiotics, structural analyses identified three different conformations of the ClpP tetradecamer: a proteolytically active, extended conformation, an inactive, compact intermediate, and an inactive, compressed conformation. The conformations all differ in the height of the ClpP barrel as well as the alignment of the catalytic triad residues (14, 59–63). The Clp protease core is understood to dynamically switch between these different conformations, thereby exhibiting separate steps of substrate hydrolysis and product release during processive substrate degradation (49, 64, 65). Here, degradation products might exit the degradation chamber through transient equatorial pores that emerge in the proteolytically inactive, compressed conformation rather than through the axial pores that may be blocked by the partner Clp-ATPases (62). Importantly, we and others have previously shown that the binding of ADEP to ClpP leads to long-distance conformational changes, thereby opening the entrance pores to the degradation chamber and locking the ClpP tetradecamer in the active, extended conformation (15, 34, 35, 38). In our current study, binding of ADEP1 led to the presence of proteolytically active ClpP1 homotetradecamers, potentially shifting ClpP1 homotetradecamers from the compressed, inactive conformation to the extended, active conformation. Also, ADEP binding stimulated proteolysis by $ClpP1P2_{hp}$ heterotetradecamers carrying a defective ClpP2 hydrophobic pocket.

Both findings clearly indicate the capacity of ADEP1 to open the entrance pores to the degradation chamber by docking to *Streptomyces* ClpP1, since this is a prerequisite for the entry of protein substrates and subsequent protein digestion (9, 10). We therefore propose the following model of ADEP action in *Streptomyces* (Fig. 6): the partner Clp-ATPase binds to the ClpP1P2 proteolytic core via ClpP2 and unfolds and feeds the natural protein substrates into the degradation chamber. The simultaneous binding of ADEP to the opposite side of the proteolytic core via ClpP1 stabilizes the core in the proteolytically active, extended conformation (including the correct arrangement of the active centers for catalysis) and stimulates the proteolysis of natural Clp substrates that are fed by the Clp-ATPase via ClpP2. This process may be further accelerated by a more efficient product release through an opened pore of the ADEP-bound ClpP1 heptamer of the proteolytically active tetradecameric core. We have previously shown that ADEP-activated EcClpP degrades largely unstructured proteins like casein with reduced processivity compared to EcClpAP (37). This may be explained by the diffusion of partially cleaved substrates through the opened axial pores in ADEP-activated EcClpP, thereby impeding processive cleavage, whereas such escape of degradation intermediates is prevented in EcClpAP (35). However, in our model for the *Streptomyces* Clp protease, Clp-ATPase-dependent processive cleavage would be allowed even in the

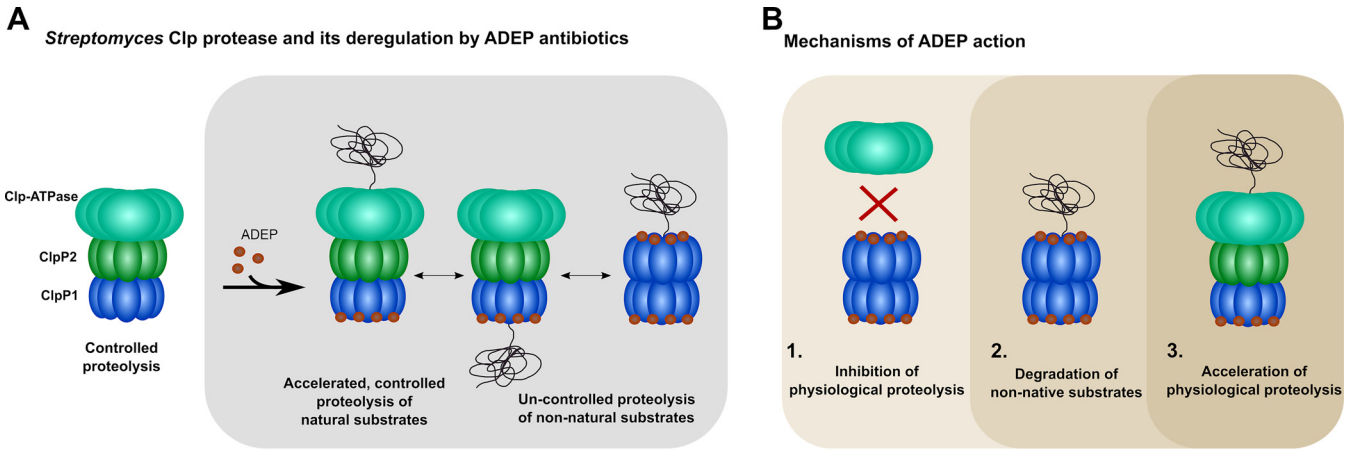

FIG 6 Mechanisms of action of ADEP antibiotics in *Streptomyces* and other bacteria. (A) Model of the housekeeping Clp protease in *Streptomyces* and its deregulation by ADEP antibiotics. The major Clp protease in *Streptomyces* is composed of a heterotetradecameric core formed by ClpP1 and ClpP2 that interacts with the AAA+ chaperones ClpX, ClpC1, or ClpC2 via ClpP2. The catalytic triad of ClpP1 is solely responsible for enzymatic hydrolysis of protein and polypeptide substrates. By binding to the ClpP1P2 proteolytic core via ClpP2, the Clp-ATPases unfold and feed natural protein substrates into the degradation chamber in an ATP-dependent manner. Simultaneous binding of ADEP can occur at the opposite side of the proteolytic core via ClpP1, which locks the core in the proteolytically active extended conformation and stimulates the proteolysis of natural Clp substrates that are fed by a Clp-ATPase via ClpP2. Binding of the antibiotic to ClpP1 also widens the ClpP1 entrance pore to allow entry of nonnative substrates into the ClpP1P2 heterotetradecamer. In addition, ADEP triggers the oligomerization of ClpP1 into a homotetradecamer, which is thereby activated for Clp-ATPase-independent proteolysis of nonnative substrates. As the presence of ClpP1 alone (i.e., in the absence of ClpP2) is sufficient to sensitize *Streptomyces* against ADEP, the degradation of nonnative protein and polypeptide substrates is the primary reason for cell death in this species. Nonetheless, while the physiological protein substrates of the Clp protease can still be degraded in the presence of ADEP, accelerated degradation of native substrates will probably also stress the cells through protein imbalance. (B) Summary of mechanisms of action of ADEP antibiotics across different bacterial species. We have previously described that ADEP antibiotics can lead to the inhibition of natural Clp protease functions (1) as well as to the uncontrolled degradation on nonnatural Clp substrates in the absence of otherwise regulating Clp-ATPases (2). We here present a third, new mechanism of ADEP action that manifests in the producer genus *Streptomyces* and leads to the acceleration of the Clp-ATPase-dependent digestion of natural Clp protease substrates (3).

presence of ADEP, potentially stimulating the degradation of natural Clp substrates. In the closely related *M. tuberculosis*, ADEP binds to only one side of the ClpP heterotetradecamer exclusively (i.e., to MtClpP2) but was shown in crystal structures to open the entrance pores on both sides of the barrel (15). Thus, it may be further hypothesized that upon binding of ADEP to *Streptomyces* ClpP1, long-distance conformational shifts might help to widen the diameter of the ClpP2 axial pore, which could additionally ease the feeding of proteins substrates by the Clp-ATPase.

Indeed, our results clearly indicate the existence of an inherent communication network between the ClpP1 and ClpP2 heptameric rings of the *Streptomyces* ClpP barrel. For example, the binding of a Clp-ATPase to ClpP2 led to catalytic stimulation of ClpP1, potentially implying an allosteric activation mechanism for ClpP1 upon concerted conformational rearrangements in both heptameric rings. In addition, self-processing of ClpP1 was induced by the binding of ClpX to ClpP2 at the opposite side of the heteromeric complex *in vitro*. Inter-ring communication is not unusual among Clp proteases studied to date (66–69). For example, Weber-Ban and colleagues (70) showed that in asymmetric *E. coli* ClpP tetradecamers, composed of one wild-type and one catalytically inactive heptameric ring, ClpA-ATPase activity could be stimulated by ClpP regardless of whether ClpA bound to the wild-type or the catalytically inactive ring. Recently, it has also been shown that the presence of catalytically active ClpP proteins is required to activate ClpA. This happens through an allosteric signal across the ClpA-ClpP interaction surface (71).

The results presented in this study unravel the composition and molecular operation mode of the *Streptomyces* housekeeping Clp protease machinery as well as its unique stimulation by ADEP antibiotics. The protein imbalance upon enhanced degradation of natural Clp substrates can be expected to cause severe cellular stress. However, the ADEP-mediated catalytic acceleration of the Clp-ATPase-controlled digestion of natural Clp substrates is not the only kind of deregulation that ADEP inflicts on the *Streptomyces* Clp protease machinery. The efficient degradation of casein by the ADEP-bound ClpP1P2

heterotetradecamer and ClpP1 homotetradecamer shows that nonnative substrates gain access to both ADEP-activated proteolytic cores, via the opened entrance pore of the ClpP1 heptameric ring. Also, *S. lividans* mutants carrying ClpP1 but lacking ClpP2 were killed by ADEP application. This illustrates that Clp-ATPase-independent and thus uncontrolled proteolysis of essential and nonessential polypeptide or protein substrates is already sufficient to cause cell death in *Streptomyces*.

MATERIALS AND METHODS

Construction of plasmids for protein expression. Plasmids for the expression of *clp*, *clgR*, and *popR* genes of *S. hawaiiensis* NRRL 15010 were obtained by ligating PCR-amplified gene sequences with linearized pET11a or pET22b vectors (Merck-Novagen), respectively. All bacterial strains, plasmids, and primers used in this study are listed in Tables S1 and S2 in the supplemental material (see also references 72–77), including a detailed description of templates and restriction enzymes used. As PCR template, genomic DNA of *S. hawaiiensis* NRRL 15010 (NCBI GenBank accession number CP021978.1) was used to amplify *shclpP1* (orf CEB94_14110), *shclpP2* (orf CEB94_14105), *shClpX* (orf CEB94_14100), *shclpC1* (orf CEB94_23085), *shclpC2* (orf CEB94_33910), *shclgR* (orf CEB94_30145), and *shpopR* (MT943519). Since *clpP2* encodes an internal XhoI restriction site, the vector pET22b*NcoI was created, in which the XhoI restriction site was exchanged for an NcoI restriction site (19). In addition, both *shclpP1* and *shclpP2* genes were cloned into the pETDUET-1 vector (Merck-Novagen), yielding the plasmid pETDUET*shclpP1*$_{ATG2}$*clpP2*-His, in which the simultaneous expression of the *clp* genes is regulated by two distinct T7 promoters. Additionally, side-directed mutagenesis was performed, yielding the constructs pET22bshclpP1$_{S113A}$, pET22bshclpP2$_{S131A}$, pET11ashclpP1$_{hp}$, pET11ashclpP1$_{Y76S}$, pET22bshclpP2$_{hp}$, and pET22bshclpP2$_{S94Y}$. Therefore, primers were designed according to the protocol of the QuikChange II Site-directed mutagenesis kit (Agilent) and as listed in Table S2. To verify the correct nucleotide sequence of the respective gene, Sanger sequencing was performed by LGC Genomics, Germany. Of note, both ClpP1 and ClpP2 were used as unprocessed proteins in all assays unless mentioned otherwise. However, during sequence analysis of ClpP2, a second putative start codon was detected, which would give rise to a shortened protein (ClpP2$_{ATG2}$). To ensure that ClpP2$_{ATG2}$ would behave similarly compared to full-length ClpP2, we also cloned and purified ClpP2$_{ATG2}$, determined its processing site, and performed degradation experiments using ClpP2 and ClpP2$_{ATG2}$ side by side. Here, no differences were observed for ClpP2$_{ATG2}$ compared to using ClpP2 (Fig. S7). Of note, due to solubility issues, ClpP2 proteins with mutations in the hydrophobic pocket (i.e., ClpP2$_{hp}$, ClpP2$_{S94Y}$) were produced from ATG2 and were then compared to ClpP2$_{ATG2}$ in respective assays (Fig. 2B to D; Fig. 3B and 3F; Fig. 5A to D; Fig. S2H, S3A, and S7).

Protein expression and purification. For the expression and purification of Clp proteins and the substrates ClgR and PopR, the respective expression plasmids were transformed into the Δ*clpP* deletion strain *E. coli* SG1146a (78). The resulting expression strains were then used to inoculate expression cultures using lysogeny broth (LB) supplemented with ampicillin (100 μg/mL). Cultures were grown at 37°C with constant shaking until a mid-log exponential growth phase (OD_{600} of 0.5 to 0.6) was reached and then protein expression was induced with 0.5 to 1 mM IPTG. Expression cultures for ClpP1, the ClpATPases, and PopR were further incubated for 4 to 5 h at 30°C with constant shaking, whereas ClpP2 and ClgR expression was carried out for 16 h at 30°C and 20°C, respectively. Then, cells were harvested by centrifugation. The following purification procedure was performed at 4°C. For cell disruption, glass beads were utilized (150 to 212 μm) in a Precellys homogenizer (Precellys evolution, Bertin technologies). Cell lysates were centrifuged, and supernatants were passed through 0.45-μm membrane filters (Sarstedt) to remove cell debris before further processing. For purification of untagged ClpP1 and ClpP2, the respective supernatants were applied to 1/5 mL HiTrap Q XL columns (GE Healthcare) for anion-exchange chromatography using the ÄKTA Start chromatography system (GE Healthcare) with buffer A (50 mM Tris, pH 8) and buffer B (50 mM Tris and 1 M NaCl, pH 8). For purification of His_6-tagged proteins, 500 to 700 μL Ni-NTA resin (Thermo-Fisher) was added to the supernatant and the suspension was incubated for at least 2 h at 4°C. Affinity chromatography was performed using lysis buffer (50 mM NaH_2PO_4, 300 mM NaCl, and 10 mM imidazole, pH 7.7), wash buffer (50 mM NaH_2PO_4, 300 mM NaCl, 20 mM imidazole, pH 7.7), and elution buffer (50 mM NaH_2PO_4, 300 mM NaCl, and 500 mM imidazole, pH 7.7). Protein fractions were pooled for buffer exchange employing a PD-10 Sephadex G-25 desalting column (GE Healthcare) and centrifugal filters (Amicon Ultracel-10 K/30 K; Merck). Protein concentration and purity were determined via SDS-PAGE analysis, Bradford assay (Bio-Rad, applying BSA as reference), and immunoblotting. Here, polyclonal rabbit anti-ClpP1 and rabbit anti-ClpP3 antibodies (provided by Philippe Mazodier) were used, which have been previously described (22–24, 36). For 6×-His-tag detection, monoclonal mouse anti-6×-His antibodies (Epitope-tag-clone HIS.H8; Thermo Fisher) were employed. Accordingly, IgG (H+L) rabbit anti-mouse horseradish peroxidase (HRP) (Invitrogen) or IgG (H+L) goat anti-rabbit HRP (Pierce) was used as secondary antibodies.

Size exclusion chromatography. To study the oligomeric behavior of native ClpP1 and native ClpP2, analytical gel filtration was performed using the Superdex 200 Increase 10/300 GL column (GE Healthcare). To this end, 80 μM of each protein was incubated with or without the addition of 200 μM ADEP1 for 30 min at 30°C. As a control, DMSO was used instead of ADEP1. Additionally, ClpP1P2$_{His}$ (90 μM each) was incubated with 200 μM ADEP1 for 2 h at 30°C and applied to the gel filtration column. For gel filtration, buffer GF was used (50 mM HEPES-KOH, 150 mM KCl, 20 mM $MgCl_2$, 10% glycerol, and 1 mM DTT, pH 7.5). The protein markers thyroglobulin (669 kDa), ferritin (440 kDa), aldolase (158 kDa), conalbumin (75 kDa), and ovalbumin (43 kDa) were employed for size estimation.

Thermal shift assays. To determine the binding affinity of ADEP1 to native ClpP1 and native ClpP2, thermal shift assays were performed. Therefore, 30 μM of each protein in GF buffer was incubated with or without the addition of 75 μM ADEP1 for 30 min at 30°C, before adding 1× SYPRO orange (Merck). DMSO was used as a control. Here, the following method was used on a QuantStudio 3 (Fisher Scientific) RT-PCR cycler: 20°C for 3 min, 20°C to 90°C with an increase of 0.05°C sec^{-1}. Baseline correction, Boltzmann sigmoid curve fitting, and fast Fourier transform curve smoothening were performed using the OriginLab software. Four replicates were analyzed. *P* values were calculated with one-way ANOVA (not significant [ns], $P > 0.05$; *, $P \leq 0.05$; **, $P \leq 0.01$; ***, $P \leq 0.001$; ****, $P \leq 0.0001$).

***In vitro* peptidase assays.** Peptidase assays were carried out in a total volume of 100 μL at 30°C in activity buffer (50 mM HEPES-KOH, 150 mM KCl, 20 mM $MgCl_2$, and 10% glycerol, pH 7.5). Peptidase activity of ClpP1 and $ClpP2_{His}$ was measured using 100 μM fluorogenic *N*-succinyl-Leu-Tyr-7-amido-4-methylcoumarin (Suc-LY-AMC), 100 μM benzyloxycarbonyl-glycyl-glycyl-L-leucine-7-amino-4-methylcoumarin (Z-GGL-AMC), 100 μM acetyl-Trp-Leu-Ala-7-amino-4-methylcoumarin (Ac-WLA-AMC), or 100 μM Ac-Ala-hArg-(*S*)-2-aminooctanoic acid-7-amino-4-carbamoylmethylcoumarin (Ac-Ala-hArg-2-Aoc-ACC) as the substrates in the absence or presence of 10 μM ADEP1. A total ClpP protein concentration of 4 μM was employed for each sample, using equal amounts of ClpP1 and ClpP2 (2 μM each) in mixed samples. Furthermore, ClpP2 (4 μM) was tested at increased concentrations of ADEP1, i.e., 100 μM and 200 μM, while ADEP-sensitive ClpP1 (4 μM) plus 100 μM ADEP1 was used as a positive control. In all assays, DMSO served as a negative control. For the analysis of the hydrophobic pocket mutants $ClpP1_{hp}$ and $ClpP2_{hp}$, a total ClpP protein concentration of 8 μM in the absence or presence of 30 μM ADEP1, ADEP2, or ADEP4 was used. ClpP and ADEP/DMSO were preincubated for 10 min at 30°C. The release of AMC (Suc-LY-AMC or Z-GGL-AMC) was monitored in black flat-bottom 96-well plates (Sarstedt) in a spectrofluorometer (TECAN Spark) at an excitation wavelength λex of 380 nm and an emission wavelength λem of 460 nm. Experiments using Ac-WLA-AMC or Ac-Ala-hArg-2-Aoc-ACC as the substrates were performed in black flat-bottom 96-well plates (Sarstedt) in a spectrofluorometer (TECAN Spark) at λex 430 nm/λem 351 nm for Ac-WLA-AMC and λex 380 nm/λem 430 nm for Ac-Ala-hArg-2-Aoc-ACC. At least three biological replicates were analyzed, each with three technical replicates, with an exception for testing $ClpP_{hp}$ mutants with two biological replicates. *P*-values were calculated with one-way ANOVA (ns, $P > 0.05$; *, $P \leq 0.05$; **, $P \leq 0.01$; ***, $P \leq 0.001$; ****, $P \leq 0.0001$).

***In vitro* casein degradation and ClpP processing assays.** For the ClpC1-mediated degradation of fluorescein isothiocyanate-casein (FITC-casein; Sigma; catalog no. c3777), 4 μM ClpC1 and a total ClpP protein concentration of 8 μM (4 μM each in mixed samples) were resuspended in activity buffer. Proteins were preincubated for 10 min at 30°C before the reaction was started by adding 6 μM FITC-casein. Mixed samples of $ClpP1P2_{His}$ in the absence of ClpC1 were tested in control reactions. Reactions were performed in the absence or presence of 30 μM ADEP1 or an equal volume of DMSO as a control. Degradation of FITC-casein (6 μM) by ClpC2P1P2 or ClpXP1P2 (4 μM each) was conducted accordingly. The hydrolysis of FITC-casein was monitored in black 96-well plates (Sarstedt) in a spectrofluorometer (Tecan Spark) at λex 490 nm/λem 525 nm. At least with three biological replicates were analyzed, each comprising three technical replicates. Statistics were performed with one-way ANOVA (ns, $P > 0.05$; *, $P \leq 0.05$; **, $P \leq 0.01$; ***, $P \leq 0.001$; ****, $P \leq 0.0001$). For the ClpC2-mediated degradation of β-casein, equal amounts of ClpP1, $ClpP2_{His}$, and ClpC2 (1.5 μM each) and 10 μM β-casein were incubated in activity buffer for 4 h at 30°C. Reactions were performed in the absence or presence of 30 μM ADEP1 or equal volume of DMSO as a control. For *in vitro* ClpP processing assays, 2 μM either ClpP1 or $ClpP2_{His}$ or mixed samples consisting of both 2 μM ClpP1 and 2 μM $ClpP2_{His}$ were incubated at 30°C with 10 μM ADEP1 or DMSO in activity buffer. Samples were taken at indicated time points and were analyzed via SDS-PAGE. Experiments were performed at least in biological triplicates, and representative SDS-PAGE images are shown. In all assays for FITC-casein and β-casein degradation, an artificial ATP regeneration system (4 mM ATP, 8 mM creatine phosphate, and 10 U/mL creatine phosphokinase) was used in the reactions to sufficiently replenish ATP for Clp-ATPase activity.

***In vitro* degradation of ClgR and PopR.** For the ClpX-mediated degradation of ClgR and PopR (3 μM each), 3 μM ClpP1 and 3 μM $ClpP2_{His}$ (or 1.5 μM each in mixed samples) were used in combination with 1.5 μM ClpX in activity buffer plus 2 mM DTT. For the ClpC1- or ClpC2-mediated degradation of ClgR and PopR (3 μM each), 1.5 μM ClpP1 and 1.5 μM $ClpP2_{His}$ were used in combination with either ClpC1 or ClpC2 (each 1.5 μM). Reactions were performed in the absence or presence of 30 μM ADEP1 or an equal volume of DMSO as a control. Experiments were performed at least in biological triplicates, and representative SDS-PAGE images are shown. An artificial ATP regeneration system (4 mM ATP, 8 mM creatine phosphate, and 10 U/mL creatine phosphokinase) was used in the reactions to sufficiently replenish ATP for Clp-ATPase activity.

Densitometry. The relative quantity of protein bands was calculated using Image Lab Software (Bio-Rad). As a reference, the protein bands collected at time point 0 h (t0) were utilized for each sample. The mean values of three biological replicates are shown.

***In vitro* degradation of GFP-ssrA.** For the ClpX-mediated degradation of C terminally ssrA-tagged GFP, 3 μM ClpP1, $ClpP2_{His}$, and ClpX were used, mixed in activity buffer plus 2 mM DTT. Reactions were performed in the absence or presence of 30 μM ADEP1 or an equal volume of DMSO as a control. An artificial ATP regeneration system was added to the reactions as described above. All reaction components except for GFP-ssrA were preincubated for 10 min at 30°C. Then, reactions were started by adding 0.36 μM GFP-ssrA. GFP fluorescence was monitored in white, flat bottom 96-well plates (Greiner) over 120 min at excitation wavelength λ ex of 465 nm and emission at λ em of 535 nm using a spectrofluorometer (TECAN infinite M200 and TECAN Spark). The data shown is exemplary for three independently performed biological replicates.

Pulldown assays. For the coelution of untagged ClpP1 with His-tagged ClpP2, *E. coli* SG1146a harboring the pETDUET-derived plasmid pETDUET*shclpP1clpP2*-His was cultured for 4 h at 30°C before coexpression of both proteins was induced by the addition of 0.5 mM IPTG. Then, cells were harvested by centrifugation and lysed, and the resulting supernatants were used for affinity chromatography as described above for His_6-tagged proteins. The flowthrough, wash, and elution fractions were sampled and analyzed via SDS-PAGE. As a control, purified ClpP1 or $ClpP2_{His}$ (8 μM each) was passed in separate runs over a nickel-NTA chromatography column, and the flowthrough, wash, and elution fractions were collected and analyzed. For immunoblotting, protein samples were transferred onto a nitrocellulose membrane (Thermo-Fisher) via semidry blotting for 1 h at 0.8 mA/cm^2. For the detection of ClpP1 and ClpP2-His_6, anti-ClpP1 (1:2,000) and anti-His_6 (1:1,000) primary antibodies were employed. HRP-coupled secondary antibodies were used and resulting chemiluminescent signals were detected via a ChemiDoc documentation system (Bio-Rad). Experiments were performed at least in biological triplicates, and representative SDS-PAGE or Western blot images are shown.

Intact-protein mass spectrometry. High-resolution intact protein mass spectrometry was performed to analyze the processing sites of ClpP1 and $ClpP2_{His}$ of *S. hawaiiensis*. Measurements were performed on a Dionex Ultimate 3000 HPLC system coupled to an LTQ FT Ultra (Thermo) mass spectrometer with an electrospray ionization source (spray voltage, 4.0 kV; tube lens, 110 V; capillary voltage, 48 V; sheath gas, 60 arbitrary units [AU]; aux gas, 10 AU; and sweep gas, 0.2 AU). Reaction mixtures containing a total of about 1 to 10 pmol protein were desalted with a Massprep desalting cartridge (Waters) before measurement. The mass spectrometer was operated in positive ion mode, collecting full scans at high resolution (R = 200,000) from m/z 600 to m/z 2,000. The protein spectra were deconvoluted using the Thermo Xcalibur Xtract algorithm.

Oligomerization studies via native PAGE. To visualize the formation of a ClpP1P2 heteromeric complex, the cross-linking reagent BS3 (bis-sulfosuccinimidyl suberate; Thermo-Fisher) was used to stabilize interactions between ClpP1 and $ClpP2_{His}$. To this end, ClpP1, ClpP2, or a mixture of both ClpP1 and ClpP2 (6 μM each) was preincubated for 30 min at 30°C in activity buffer. For cross-linking reactions, a 50-fold molar excess of BS3 over the total ClpP concentration (6 mM BS3 for the mixed ClpP1P2 samples, or 3 mM BS3 for samples with either ClpP1 or ClpP2) was added to the samples. Reaction mixtures were incubated for 30 min at 30°C without shaking. Subsequently, the reactions were stopped by adding 20 mM Tris to the samples followed by further incubation for 15 min at room temperature. For analyzing the oligomeric behavior in the presence of ADEP1, ClpP1 and ClpP2 (10 μM each) were incubated with 60 μM ADEP1 (ClpP:ADEP1 ratio of 1:3) or 25 μM ADEP1 (ClpP:ADEP1 ratio of 1:1.25) for 3 h at 30°C. DMSO was used as a negative control. Samples were subjected to native PAGE at 25 V for approximately 16 h at 4°C. Gels were either Coomassie stained or used for immunoblotting employing PVDF membranes (Merck) as described above. To visualize a heteromeric ClpP1P2 complex, cross-linking experiments were conducted using the following activity buffer: 50 mM HEPES, 200 mM $Na_3C_6H_5O_7$, 20 mM $MgCl_2$, and 10% glycerol, pH 7.5. The experiment was performed with ClpP1P2 (10 or 15 μM each), which were incubated for 30 min at 30°C with ADEP1 (25 μM or 37.5 μM, respectively). Then, a 50-fold molar excess of BS3 over the total ClpP concentration was added to the samples and incubated for 30 min at 30°C. Samples were analyzed via native PAGE, using 4–12% Tris-glycine precast gels and ready-mixed native sample buffer (both Thermo-Fisher). Immunoblotting was performed as described above except for using PVDF membranes.

ATPase activity. The ADP-Glo kinase assay (Promega) was utilized to measure the turn-over of ATP to ADP in ClpC1-mediated casein degradation assays according to the manufacturer's instructions. In the first step, the reaction was conducted using $ClpP1P2_{His}$ (8 μM each), ClpC1 (8 μM), β-casein (10 μM) as a substrate, as well as ultrapure ATP (100 nM; Promega). After 60 min of incubation at 30°C, the reaction was stopped by adding ADP-Glo reagent to deplete the remaining ATP. ATP depletion was carried out for 40 min at room temperature. In a second step, the Kinase Detection Reagent was added for the conversion of ADP to ATP and incubated for 1 h at RT using a 384-well plate. In 384-well plates, 5 μL reaction mixture, 5 μL ADP-Glo reagent, and 10 μL of Kinase Detection Reagent were used. The converted ATP was then measured via a luciferase/luciferin reaction and ADP-Glo kinase assay luminescence was recorded.

Bacterial strains, culture conditions, and cloning procedures for cell-based studies. All bacterial strains, plasmids, and primers used in this study are listed in Tables S1 and S2. *Streptomyces* wild-type and mutant strains were grown at 30°c on ms-$mgcl_2$ agar (2% soy flour, 2% mannitol, 2% agar, 10 mm $mgcl_2$) or in tryptic soy broth (TSB; BD Biosciences) with apramycin (50 μg/mL) and/or hygromycin B (50 μg/mL) as appropriate. *E. coli* strains were propagated in LB medium with apramycin (50 μg/mL), hygromycin B (50 μg/mL), kanamycin (25 μg/mL), and/or chloramphenicol (30 μg/mL) as required. For cloning purposes, DNA fragments of the genes of interest were PCR amplified and cloned into the respective vector via restriction-ligation utilizing *E. coli* JM109 or *E. coli* DH5α as cloning strains. All constructs were verified by Sanger sequencing (LGC Genomics). *Streptomyces* vectors were conjugated into the respective *Streptomyces* strains via *E. coli* ET12567 pUB307 as described previously (79). Site-directed mutagenesis was performed as described above. For the generation of *clpP* deletion mutants, markerless gene knockouts were achieved by PCR-amplifying 1.5-kb long flanking regions of the respective gene, which were then integrated into the pGM-GUS-Xba vector by Gibson assembly using the NEBuilder HiFi DNA Assembly Master Mix (NEB) and *E. coli* JM109 or *E. coli* DH5α as cloning hosts. After verification by Sanger sequencing, the knockout constructs were transformed into *E. coli* ET12567 pUB307 and conjugated into *S. lividans* TK24 as described previously (79). Mutant colonies were grown with apramycin at 39°C in TSB liquid cultures and subsequently on MS agar to maintain cells with integrated plasmids only. Spores were harvested and dilutions were plated on LB agar with 2 μg/mL of ADEP1 as selective pressure for plasmid loss. The obtained colonies were overlaid with 1 mL of an X-Gluc (5-bromo-4-chloro-3-indolyl-β-D-glucuronide) solution in water (1 mg/mL) for a blue-white screen. For white colonies, loss of the vector and the respective *clpP* gene was further verified by colony PCR and subsequent Sanger sequencing. Multiple sequence alignments were generated with the online tool clustalΩ (https://www.ebi.ac.uk/Tools/msa/clustalo/). Sequence identities were computed using Jalview Software (80).

ADEP sensitivity assays. Spore suspensions of the respective *Streptomyces* strains were plated on nutrient extract agar (1% glucose, 0.2% yeast extract, 0.2% Casamino Acids, and 0.1% Lab-Lemco Powder, pH 7.0). Paper disks containing 20 μg of ADEP1 were added to the plates, which were subsequently incubated at 30°C for 2 days.

Preparation of *Streptomyces* culture protein extracts. The respective *Streptomyces* strains were grown in 10 mL of TSB medium with apramycin and/or hygromycin as appropriate for 40 h at 30°C and 180 rpm. The mycelium was harvested and resuspended in 500 μL of lysis buffer (20 mM Tris, 5 mM EDTA disodium salt, 1 mM 2-mercaptoethanol; one cOmplete Mini, EDTA-free protease inhibitor cocktail tablet [Roche] per 10 mL of lysis buffer) in 2-mL lysis tubes. Upon cell disruption using the Precellys homogenizer, cell debris was removed by two centrifugation steps (14,000 rpm, 10 min, 4°C followed by 14,000 rpm, 20 min, 4°C), and the concentration of the protein extracts was determined by measuring the absorption at 280 nm with the NanoDrop 2000c spectrophotometer (Thermo Scientific).

SUPPLEMENTAL MATERIAL

Supplemental material is available online only.

FIG S1, PDF file, 2.6 MB.
FIG S2, PDF file, 0.7 MB.
FIG S3, PDF file, 0.6 MB.
FIG S4, PDF file, 2.5 MB.
FIG S5, PDF file, 0.3 MB.
FIG S6, PDF file, 0.9 MB.
FIG S7, PDF file, 1.3 MB.
TABLE S1, PDF file, 0.1 MB.
TABLE S2, PDF file, 0.1 MB.

ACKNOWLEDGMENTS

We are grateful to all members of our teams and the RTG 1708 and TRR 261 for their support and critical discussions. Further, we thank Philippe Mazodier for the kind gift of antibodies, Günther Muth and Susan Gottesman for providing the bacterial strains *S. lividans* TK24 and *E. coli* SG1146a, respectively, and Marc Buttner for sharing the plasmids pIJ12551 and pIJ10257. We also acknowledge the technical support of Stefan Pan, Janna Hauser, and Denijel Latifovic.

L. Reinhardt, D. Thomy, P. Sass, and H. Brötz-Oesterhelt designed the study. L. Reinhardt and D. Thomy conducted all experiments with the exception of intact-protein mass spectrometry. M. Lakemeyer and S. Sieber performed intact-protein mass spectrometry. J. Ortega contributed materials, plasmids, and techniques. L. Reinhardt, D. Thomy, M. Lakemeyer, P. Sass, and H. Brötz-Oesterhelt analyzed data. P. Sass and H. Brötz-Oesterhelt supervised the study. L. Reinhardt, D. Thomy, and P. Sass prepared figures and drafted the manuscript. All authors finalized and approved the manuscript. P. Sass and H. Brötz-Oesterhelt acquired funding.

The authors appreciate funding from the Deutsche Forschungsgemeinschaft (DFG; German Research Foundation): Project-ID 174858087 (RTG 1708, project B5) and Project-ID 398967434 (TRR 261, projects A01 and A02), as well as support by infrastructural funding from Cluster of Excellence EXC 2124 Controlling Microbes to Fight Infections, (Project-ID 390838134). We further acknowledge financial support by the University of Düsseldorf/ Research Centre Jülich (iGRASPseed fellowship to D. Thomy) and by the Open Access Publishing Fund of the University of Tübingen.

The authors have declared that no competing interests exist.

REFERENCES

1. Flärdh K, Buttner MJ. 2009. Streptomyces morphogenetics: dissecting differentiation in a filamentous bacterium. Nat Rev Microbiol 7:36–49. https://doi.org/10.1038/nrmicro1968.
2. Illigmann A, Thoma Y, Pan S, Reinhardt L, Brötz-Oesterhelt H. 2021. Contribution of the Clp protease to bacterial survival and mitochondrial homoeostasis. Microb Physiol 31:260–279. https://doi.org/10.1159/000517718.
3. de Crecy-Lagard V, Servant-Moisson P, Viala J, Grandvalet C, Mazodier P. 1999. Alteration of the synthesis of the Clp ATP-dependent protease affects morphological and physiological differentiation in Streptomyces. Mol Microbiol 32:505–517. https://doi.org/10.1046/j.1365-2958.1999.01364.x.
4. Wolanski M, Donczew R, Kois-Ostrowska A, Masiewicz P, Jakimowicz D, Zakrzewska-Czerwinska J. 2011. The level of AdpA directly affects expression of developmental genes in Streptomyces coelicolor. J Bacteriol 193:6358–6365. https://doi.org/10.1128/JB.05734-11.
5. Guyet A, Gominet M, Benaroudj N, Mazodier P. 2013. Regulation of the clpP1clpP2 operon by the pleiotropic regulator AdpA in Streptomyces

lividans. Arch Microbiol 195:831–841. https://doi.org/10.1007/s00203-013-0918-2.
6. Guyet A, Benaroudj N, Proux C, Gominet M, Coppee JY, Mazodier P. 2014. Identified members of the Streptomyces lividans AdpA regulon involved in differentiation and secondary metabolism. BMC Microbiol 14:81. https://doi.org/10.1186/1471-2180-14-81.
7. Olivares AO, Baker TA, Sauer RT. 2016. Mechanistic insights into bacterial AAA+ proteases and protein-remodelling machines. Nat Rev Microbiol 14:33–44. https://doi.org/10.1038/nrmicro.2015.4.
8. Wang J, Hartling JA, Flanagan JM. 1997. The structure of ClpP at 2.3 A resolution suggests a model for ATP-dependent proteolysis. Cell 91:447–456. https://doi.org/10.1016/S0092-8674(00)80431-6.
9. Woo KM, Chung WJ, Ha DB, Goldberg AL, Chung CH. 1989. Protease Ti from Escherichia coli requires ATP hydrolysis for protein breakdown but not for hydrolysis of small peptides. J Biol Chem 264:2088–2091. https://doi.org/10.1016/S0021-9258(18)94145-1.
10. Thompson MW, Maurizi MR. 1994. Activity and specificity of Escherichia coli ClpAP protease in cleaving model peptide substrates. J Biol Chem 269:18201–18208. https://doi.org/10.1016/S0021-9258(17)32435-3.
11. Kirstein J, Molière N, Dougan DA, Turgay K. 2009. Adapting the machine: adaptor proteins for Hsp100/Clp and AAA+ proteases. Nat Rev Microbiol 7:589–599. https://doi.org/10.1038/nrmicro2185.
12. Gribun A, Kimber MS, Ching R, Sprangers R, Fiebig KM, Houry WA. 2005. The ClpP double ring tetradecameric protease exhibits plastic ring-ring interactions, and the N termini of its subunits form flexible loops that are essential for ClpXP and ClpAP complex formation. J Biol Chem 280:16185–16196. https://doi.org/10.1074/jbc.M414124200.
13. Lee BG, Kim MK, Song HK. 2011. Structural insights into the conformational diversity of ClpP from Bacillus subtilis. Mol Cells 32:589–595. https://doi.org/10.1007/s10059-011-0197-1.
14. Gersch M, List A, Groll M, Sieber SA. 2012. Insights into structural network responsible for oligomerization and activity of bacterial virulence regulator caseinolytic protease P (ClpP) protein. J Biol Chem 287:9484–9494. https://doi.org/10.1074/jbc.M111.336222.
15. Schmitz KR, Carney DW, Sello JK, Sauer RT. 2014. Crystal structure of Mycobacterium tuberculosis ClpP1P2 suggests a model for peptidase activation by AAA+ partner binding and substrate delivery. Proc Natl Acad Sci U S A 111:E4587–4595. https://doi.org/10.1073/pnas.1417120111.
16. Dahmen M, Vielberg MT, Groll M, Sieber SA. 2015. Structure and mechanism of the caseinolytic protease ClpP1/2 heterocomplex from Listeria monocytogenes. Angew Chem Int Ed Engl 54:3598–3602. https://doi.org/10.1002/anie.201409325.
17. Hall BM, Breidenstein EBM, de la Fuente-Nunez C, Reffuveille F, Mawla GD, Hancock REW, Baker TA. 2017. Two isoforms of Clp peptidase in Pseudomonas aeruginosa control distinct aspects of cellular physiology. J Bacteriol 199:e00568-16. https://doi.org/10.1128/JB.00568-16.
18. Lavey NP, Shadid T, Ballard JD, Duerfeldt AS. 2019. Clostridium difficile ClpP Homologues are capable of uncoupled activity and exhibit different levels of susceptibility to acyldepsipeptide modulation. ACS Infect Dis 5:79–89. https://doi.org/10.1021/acsinfecdis.8b00199.
19. Pan S, Malik IT, Thomy D, Henrichfreise B, Sass P. 2019. The functional ClpXP protease of Chlamydia trachomatis requires distinct clpP genes from separate genetic loci. Sci Rep 9:14129. https://doi.org/10.1038/s41598-019-50505-5.
20. Nagpal J, Paxman JJ, Zammit JE, Alhuwaider A, Truscott KN, Heras B, Dougan DA. 2019. Molecular and structural insights into an asymmetric proteolytic complex (ClpP1P2) from Mycobacterium smegmatis. Sci Rep 9:18019. https://doi.org/10.1038/s41598-019-53736-8.
21. Viala J, Rapoport G, Mazodier P. 2000. The clpP multigenic family in Streptomyces lividans: conditional expression of the clpP3 clpP4 operon is controlled by PopR, a novel transcriptional activator. Mol Microbiol 38:602–612. https://doi.org/10.1046/j.1365-2958.2000.02155.x.
22. Viala J, Mazodier P. 2002. ClpP-dependent degradation of PopR allows tightly regulated expression of the clpP3 clpP4 operon in Streptomyces lividans. Mol Microbiol 44:633–643. https://doi.org/10.1046/j.1365-2958.2002.02907.x.
23. Bellier A, Gominet M, Mazodier P. 2006. Post-translational control of the Streptomyces lividans ClgR regulon by ClpP. Microbiology (Reading) 152:1021–1027. https://doi.org/10.1099/mic.0.28564-0.
24. Bellier A, Mazodier P. 2004. ClgR, a novel regulator of clp and lon expression in Streptomyces. J Bacteriol 186:3238–3248. https://doi.org/10.1128/JB.186.10.3238-3248.2004.
25. Kim MS, Hahn MY, Cho Y, Cho SN, Roe JH. 2009. Positive and negative feedback regulatory loops of thiol-oxidative stress response mediated by an unstable isoform of sigmaR in actinomycetes. Mol Microbiol 73:815–825. https://doi.org/10.1111/j.1365-2958.2009.06824.x.
26. Thomy D, Culp E, Adamek M, Cheng EY, Ziemert N, Wright GD, Sass P, Brötz-Oesterhelt H. 2019. The ADEP biosynthetic gene cluster in *Streptomyces hawaiiensis* NRRL 15010 reveals an accessory clpP gene as a novel antibiotic resistance factor. Appl Environ Microbiol 85:e01292-19. https://doi.org/10.1128/AEM.01292-19.
27. Brötz-Oesterhelt H, Beyer D, Kroll HP, Endermann R, Ladel C, Schroeder W, Hinzen B, Raddatz S, Paulsen H, Henninger K, Bandow JE, Sahl HG, Labischinski H. 2005. Dysregulation of bacterial proteolytic machinery by a new class of antibiotics. Nat Med 11:1082–1087. https://doi.org/10.1038/nm1306.
28. Malik IT, Brötz-Oesterhelt H. 2017. Conformational control of the bacterial Clp protease by natural product antibiotics. Nat Prod Rep 34:815–831. https://doi.org/10.1039/C6NP00125D.
29. Mayer C, Sass P, Brötz-Oesterhelt H. 2019. Consequences of dosing and timing on the antibacterial effects of ADEP antibiotics. Int J Med Microbiol 309:151329. https://doi.org/10.1016/j.ijmm.2019.151329.
30. Silber N, Pan S, Schakermann S, Mayer C, Brötz-Oesterhelt H, Sass P. 2020. Cell division protein FtsZ is unfolded for N-terminal degradation by antibiotic-activated ClpP. mBio 11:e01006-20. https://doi.org/10.1128/mBio.01006-20.
31. Brötz-Oesterhelt H, Vorbach A. 2021. Reprogramming of the caseinolytic protease by ADEP antibiotics: molecular mechanism, cellular consequences, therapeutic potential. Front Mol Biosci 8:690902. https://doi.org/10.3389/fmolb.2021.690902.
32. Zeiler E, List A, Alte F, Gersch M, Wachtel R, Poreba M, Drag M, Groll M, Sieber SA. 2013. Structural and functional insights into caseinolytic proteases reveal an unprecedented regulation principle of their catalytic triad. Proc Natl Acad Sci U S A 110:11302–11307. https://doi.org/10.1073/pnas.1219125110.
33. Leodolter J, Warweg J, Weber-Ban E. 2015. The Mycobacterium tuberculosis ClpP1P2 protease interacts asymmetrically with its ATPase partners ClpX and ClpC1. PLoS One 10:e0125345. https://doi.org/10.1371/journal.pone.0125345.
34. Lee BG, Park EY, Lee KE, Jeon H, Sung KH, Paulsen H, Rubsamen-Schaeff H, Brötz-Oesterhelt H, Song HK. 2010. Structures of ClpP in complex with acyldepsipeptide antibiotics reveal its activation mechanism. Nat Struct Mol Biol 17:471–478. https://doi.org/10.1038/nsmb.1787.
35. Li DH, Chung YS, Gloyd M, Joseph E, Ghirlando R, Wright GD, Cheng YQ, Maurizi MR, Guarne A, Ortega J. 2010. Acyldepsipeptide antibiotics induce the formation of a structured axial channel in ClpP: a model for the ClpX/ClpA-bound state of ClpP. Chem Biol 17:959–969. https://doi.org/10.1016/j.chembiol.2010.07.008.
36. Gominet M, Seghezzi N, Mazodier P. 2011. Acyl depsipeptide (ADEP) resistance in Streptomyces. Microbiology (Reading) 157:2226–2234. https://doi.org/10.1099/mic.0.048454-0.
37. Kirstein J, Hoffmann A, Lilie H, Schmidt R, Rubsamen-Waigmann H, Brötz-Oesterhelt H, Mogk A, Turgay K. 2009. The antibiotic ADEP reprogrammes ClpP, switching it from a regulated to an uncontrolled protease. EMBO Mol Med 1:37–49. https://doi.org/10.1002/emmm.200900002.
38. Gersch M, Famulla K, Dahmen M, Gobl C, Malik I, Richter K, Korotkov VS, Sass P, Rubsamen-Schaeff H, Madl T, Brötz-Oesterhelt H, Sieber SA. 2015. AAA+ chaperones and acyldepsipeptides activate the ClpP protease via conformational control. Nat Commun 6:6320. https://doi.org/10.1038/ncomms7320.
39. Famulla K, Sass P, Malik I, Akopian T, Kandror O, Alber M, Hinzen B, Ruebsamen-Schaeff H, Kalscheuer R, Goldberg AL, Brötz-Oesterhelt H. 2016. Acyldepsipeptide antibiotics kill mycobacteria by preventing the physiological functions of the ClpP1P2 protease. Mol Microbiol 101:194–209. https://doi.org/10.1111/mmi.13362.
40. Amor AJ, Schmitz KR, Sello JK, Baker TA, Sauer RT. 2016. Highly dynamic interactions maintain kinetic stability of the ClpXP protease during the ATP-fueled mechanical cycle. ACS Chem Biol 11:1552–1560. https://doi.org/10.1021/acschembio.6b00083.
41. Gottesman S, Roche E, Zhou Y, Sauer RT. 1998. The ClpXP and ClpAP proteases degrade proteins with carboxy-terminal peptide tails added by the SsrA-tagging system. Genes Dev 12:1338–1347. https://doi.org/10.1101/gad.12.9.1338.
42. Flynn JM, Levchenko I, Seidel M, Wickner SH, Sauer RT, Baker TA. 2001. Overlapping recognition determinants within the ssrA degradation tag allow modulation of proteolysis. Proc Natl Acad Sci U S A 98:10584–10589. https://doi.org/10.1073/pnas.191375298.
43. Procopio RE, Silva IR, Martins MK, Azevedo JL, Araujo JM. 2012. Antibiotics produced by Streptomyces. Braz J Infect Dis 16:466–471. https://doi.org/10.1016/j.bjid.2012.08.014.

44. Mahmoud SA, Chien P. 2018. Regulated proteolysis in bacteria. Annu Rev Biochem 87:677–696. https://doi.org/10.1146/annurev-biochem-062917-012848.
45. Viala J, Mazodier P. 2003. The ATPase ClpX is conditionally involved in the morphological differentiation of Streptomyces lividans. Mol Genet Genomics 268:563–569. https://doi.org/10.1007/s00438-002-0783-1.
46. Martin A, Baker TA, Sauer RT. 2007. Distinct static and dynamic interactions control ATPase-peptidase communication in a AAA+ protease. Mol Cell 27:41–52. https://doi.org/10.1016/j.molcel.2007.05.024.
47. Akopian T, Kandror O, Raju RM, Unnikrishnan M, Rubin EJ, Goldberg AL. 2012. The active ClpP protease from M. tuberculosis is a complex composed of a heptameric ClpP1 and a ClpP2 ring. EMBO J 31:1529–1541. https://doi.org/10.1038/emboj.2012.5.
48. Raju RM, Unnikrishnan M, Rubin DH, Krishnamoorthy V, Kandror O, Akopian TN, Goldberg AL, Rubin EJ. 2012. Mycobacterium tuberculosis ClpP1 and ClpP2 function together in protein degradation and are required for viability in vitro and during infection. PLoS Pathog 8:e1002511. https://doi.org/10.1371/journal.ppat.1002511.
49. Gatsogiannis C, Balogh D, Merino F, Sieber SA, Raunser S. 2019. Cryo-EM structure of the ClpXP protein degradation machinery. Nat Struct Mol Biol 26:946–954. https://doi.org/10.1038/s41594-019-0304-0.
50. Sass P, Brötz-Oesterhelt H. 2013. Bacterial cell division as a target for new antibiotics. Curr Opin Microbiol 16:522–530. https://doi.org/10.1016/j.mib.2013.07.006.
51. Sass P, Josten M, Famulla K, Schiffer G, Sahl HG, Hamoen L, Brötz-Oesterhelt H. 2011. Antibiotic acyldepsipeptides activate ClpP peptidase to degrade the cell division protein FtsZ. Proc Natl Acad Sci U S A 108:17474–17479. https://doi.org/10.1073/pnas.1110385108.
52. Alexopoulos J, Ahsan B, Homchaudhuri L, Husain N, Cheng YQ, Ortega J. 2013. Structural determinants stabilizing the axial channel of ClpP for substrate translocation. Mol Microbiol 90:167–180. https://doi.org/10.1111/mmi.12356.
53. Silber N, Matos de Opitz CL, Mayer C, Sass P. 2020. Cell division protein FtsZ: from structure and mechanism to antibiotic target. Future Microbiol 15:801–831. https://doi.org/10.2217/fmb-2019-0348.
54. Silber N, Mayer C, Matos de Opitz CL, Sass P. 2021. Progression of the late-stage divisome is unaffected by the depletion of the cytoplasmic FtsZ pool. Commun Biol 4:270. https://doi.org/10.1038/s42003-021-01789-9.
55. Zeiler E, Korotkov VS, Lorenz-Baath K, Böttcher T, Sieber SA. 2012. Development and characterization of improved β-lactone-based anti-virulence drugs targeting ClpP. Bioorg Med Chem 20:583–591. https://doi.org/10.1016/j.bmc.2011.07.047.
56. Malik IT, Pereira R, Vielberg MT, Mayer C, Straetener J, Thomy D, Famulla K, Castro H, Sass P, Groll M, Brötz-Oesterhelt H. 2020. Functional characterisation of ClpP mutations conferring resistance to acyldepsipeptide antibiotics in Firmicutes. Chembiochem 21:1997–2012. https://doi.org/10.1002/cbic.201900787.
57. Raju RM, Jedrychowski MP, Wei JR, Pinkham JT, Park AS, O'Brien K, Rehren G, Schnappinger D, Gygi SP, Rubin EJ. 2014. Post-translational regulation via Clp protease is critical for survival of Mycobacterium tuberculosis. PLoS Pathog 10:e1003994. https://doi.org/10.1371/journal.ppat.1003994.
58. Culp EJ, Sychantha D, Hobson C, Pawlowski AC, Prehna G, Wright GD. 2022. ClpP inhibitors are produced by a widespread family of bacterial gene clusters. Nat Microbiol 7:451–462. https://doi.org/10.1038/s41564-022-01073-4.
59. Zhang J, Ye F, Lan L, Jiang H, Luo C, Yang CG. 2011. Structural switching of Staphylococcus aureus Clp protease: a key to understanding protease dynamics. J Biol Chem 286:37590–37601. https://doi.org/10.1074/jbc.M111.277848.
60. Geiger SR, Bottcher T, Sieber SA, Cramer P. 2011. A conformational switch underlies ClpP protease function. Angew Chem Int Ed Engl 50:5749–5752. https://doi.org/10.1002/anie.201100666.
61. Liu K, Ologbenla A, Houry WA. 2014. Dynamics of the ClpP serine protease: a model for self-compartmentalized proteases. Crit Rev Biochem Mol Biol 49:400–412. https://doi.org/10.3109/10409238.2014.925421.
62. Sprangers R, Gribun A, Hwang PM, Houry WA, Kay LE. 2005. Quantitative NMR spectroscopy of supramolecular complexes: dynamic side pores in ClpP are important for product release. Proc Natl Acad Sci U S A 102:16678–16683. https://doi.org/10.1073/pnas.0507370102.
63. Ye F, Zhang J, Liu H, Hilgenfeld R, Zhang R, Kong X, Li L, Lu J, Zhang X, Li D, Jiang H, Yang CG, Luo C. 2013. Helix unfolding/refolding characterizes the functional dynamics of Staphylococcus aureus Clp protease. J Biol Chem 288:17643–17653. https://doi.org/10.1074/jbc.M113.452714.
64. Kimber MS, Yu AY, Borg M, Leung E, Chan HS, Houry WA. 2010. Structural and theoretical studies indicate that the cylindrical protease ClpP samples extended and compact conformations. Structure 18:798–808. https://doi.org/10.1016/j.str.2010.04.008.
65. Ripstein ZA, Vahidi S, Houry WA, Rubinstein JL, Kay LE. 2020. A processive rotary mechanism couples substrate unfolding and proteolysis in the ClpXP degradation machinery. Elife 9:e52158. https://doi.org/10.7554/eLife.52158.
66. Ortega J, Lee HS, Maurizi MR, Steven AC. 2002. Alternating translocation of protein substrates from both ends of ClpXP protease. EMBO J 21:4938–4949. https://doi.org/10.1093/emboj/cdf483.
67. Ishikawa T, Beuron F, Kessel M, Wickner S, Maurizi MR, Steven AC. 2001. Translocation pathway of protein substrates in ClpAP protease. Proc Natl Acad Sci U S A 98:4328–4333. https://doi.org/10.1073/pnas.081543698.
68. Joshi SA, Hersch GL, Baker TA, Sauer RT. 2004. Communication between ClpX and ClpP during substrate processing and degradation. Nat Struct Mol Biol 11:404–411. https://doi.org/10.1038/nsmb752.
69. Vahidi S, Ripstein ZA, Juravsky JB, Rennella E, Goldberg AL, Mittermaier AK, Rubinstein JL, Kay LE. 2020. An allosteric switch regulates Mycobacterium tuberculosis ClpP1P2 protease function as established by cryo-EM and methyl-TROSY NMR. Proc Natl Acad Sci U S A 117:5895–5906. https://doi.org/10.1073/pnas.1921630117.
70. Maglica Z, Kolygo K, Weber-Ban E. 2009. Optimal efficiency of ClpAP and ClpXP chaperone-proteases is achieved by architectural symmetry. Structure 17:508–516. https://doi.org/10.1016/j.str.2009.02.014.
71. Maurizi MR. 1991. ATP-promoted interaction between Clp A and Clp P in activation of Clp protease from Escherichia coli. Biochem Soc Trans 19:719–723. https://doi.org/10.1042/bst0190719.
72. Yanisch-Perron C, Vieira J, Messing J. 1985. Improved M13 phage cloning vectors and host strains: nucleotide sequences of the M13mp18 and pUC19 vectors. Gene 33:103–119. https://doi.org/10.1016/0378-1119(85)90120-9.
73. Bennett PM, Grinsted J, Richmond MH. 1977. Transposition of TnA does not generate deletions. Mol Gen Genet 154:205–211. https://doi.org/10.1007/BF00330839.
74. Flett F, Mersinias V, Smith CP. 1997. High efficiency intergeneric conjugal transfer of plasmid DNA from Escherichia coli to methyl DNA-restricting streptomycetes. FEMS Microbiol Lett 155:223–229. https://doi.org/10.1111/j.1574-6968.1997.tb13882.x.
75. Hopwood DA, Kieser T, Wright HM, Bibb MJ. 1983. Plasmids, recombination and chromosome mapping in Streptomyces lividans 66. J Gen Microbiol 129:2257–2269. https://doi.org/10.1099/00221287-129-7-2257.
76. Sherwood EJ, Hesketh AR, Bibb MJ. 2013. Cloning and analysis of the planosporicin lantibiotic biosynthetic gene cluster of Planomonospora alba. J Bacteriol 195:2309–2321. https://doi.org/10.1128/JB.02291-12.
77. Hong HJ, Hutchings MI, Hill LM, Buttner MJ. 2005. The role of the novel Fem protein VanK in vancomycin resistance in Streptomyces coelicolor. J Biol Chem 280:13055–13061. https://doi.org/10.1074/jbc.M413801200.
78. Maurizi MR, Clark WP, Katayama Y, Rudikoff S, Pumphrey J, Bowers B, Gottesman S. 1990. Sequence and structure of Clp P, the proteolytic component of the ATP-dependent Clp protease of Escherichia coli. J Biol Chem 265:12536–12545. https://doi.org/10.1016/S0021-9258(19)38378-4.
79. Mazodier P, Petter R, Thompson C. 1989. Intergeneric conjugation between Escherichia coli and Streptomyces species. J Bacteriol 171:3583–3585. https://doi.org/10.1128/jb.171.6.3583-3585.1989.
80. Waterhouse AM, Procter JB, Martin DMA, Clamp M, Barton GJ. 2009. Jalview Version 2—a multiple sequence alignment editor and analysis workbench. Bioinformatics 25:1189–1191. https://doi.org/10.1093/bioinformatics/btp033.